The Journal of Experimental Biology 203, 2667–2689 (2000)
Printed in Great Britain © The Company of Biologists Limited 2000
JEB2869

POWER OUTPUT BY AN ASYNCHRONOUS FLIGHT MUSCLE FROM A BEETLE

ROBERT K. JOSEPHSON[1,*], JEAN G. MALAMUD[1] AND DARRELL R. STOKES[2]

[1]*School of Biological Sciences, University of California, Irvine, CA 92697, USA* and [2]*Department of Biology, Emory University, Atlanta, GA 30322, USA*

*e-mail: rkjoseph@uci.edu

Accepted 13 June; published on WWW 9 August 2000

Summary

The basalar muscle of the beetle *Cotinus mutabilis* is a large, fibrillar flight muscle composed of approximately 90 fibers. The paired basalars together make up approximately one-third of the mass of the power muscles of flight. Changes in twitch force with changing stimulus intensity indicated that a basalar muscle is innervated by at least five excitatory axons and at least one inhibitory axon. The muscle is an asynchronous muscle; during normal oscillatory operation there is not a 1:1 relationship between muscle action potentials and contractions. During tethered flight, the wing-stroke frequency was approximately 80 Hz, and the action potential frequency in individual motor units was approximately 20 Hz. As in other asynchronous muscles that have been examined, the basalar is characterized by high passive tension, low tetanic force and long twitch duration.

Mechanical power output from the basalar muscle during imposed, sinusoidal strain was measured by the work-loop technique. Work output varied with strain amplitude, strain frequency, the muscle length upon which the strain was superimposed, muscle temperature and stimulation frequency. When other variables were at optimal values, the optimal strain for work per cycle was approximately 5 %, the optimal frequency for work per cycle approximately 50 Hz and the optimal frequency for mechanical power output 60–80 Hz. Optimal strain decreased with increasing cycle frequency and increased with muscle temperature. The curve relating work output and strain was narrow. At frequencies approximating those of flight, the width of the work *versus* strain curve, measured at half-maximal work, was 5 % of the resting muscle length. The optimal muscle length for work output was shorter than that at which twitch and tetanic tension were maximal. Optimal muscle length decreased with increasing strain. The curve relating work output and muscle length, like that for work *versus* strain, was narrow, with a half-width of approximately 3 % at the normal flight frequency. Increasing the frequency with which the muscle was stimulated increased power output up to a plateau, reached at approximately 100 Hz stimulation frequency (at 35 °C). The low lift generated by animals during tethered flight is consistent with the low frequency of muscle action potentials in motor units of the wing muscles. The optimal oscillatory frequency for work per cycle increased with muscle temperature over the temperature range tested (25–40 °C). When cycle frequency was held constant, the work per cycle rose to an optimum with increasing temperature and then declined. We propose that there is a temperature optimum for work output because increasing temperature increases the shortening velocity of the muscle, which increases the rate of positive work output during shortening, but also decreases the durations of the stretch activation and shortening deactivation that underlie positive work output, the effect of temperature on shortening velocity being dominant at lower temperatures and the effect of temperature on the time course of activation and deactivation being dominant at higher temperatures.

The average wing-stroke frequency during free flight was 94 Hz, and the thoracic temperature was 35 °C. The mechanical power output at the measured values of wing-stroke frequency and thoracic temperature during flight, and at optimal muscle length and strain, averaged 127 W kg^{-1} muscle, with a maximum value of 200 W kg^{-1}. The power output from this asynchronous flight muscle was approximately twice that measured with similar techniques from synchronous flight muscle of insects, supporting the hypothesis that asynchronous operation has been favored by evolution in flight systems of different insect groups because it allows greater power output at the high contraction frequencies of flight.

Key words: asynchronous muscle, work, power, beetle, *Cotinus mutabilis*, insect, flight.

Introduction

Animals have evolved two rather different solutions to the task of providing muscles that can operate at high contraction frequencies: a quantitative solution, which is based on the speeding up of time-consuming steps in muscle activation and

relaxation, and a qualitative solution in which some of the time-consuming steps are totally bypassed. The quantitative solution is that found in muscles in which there is a 1:1 correspondence between muscle action potentials and muscle contraction, and for that reason are called synchronous muscles. The qualitative solution is found in asynchronous muscles, muscles in which there is no strict congruence between electrical and mechanical activity.

Each contraction of a synchronous muscle is initiated by action potentials or bursts of action potentials in the motor neurons to the participating fibers. The motor neuron action potentials trigger muscle fiber action potentials which, in turn, trigger the release of Ca^{2+} into the muscle cytoplasm from the sarcoplasmic reticulum. The released Ca^{2+} binds to control sites and activates the contractile myofibrils. High-frequency, synchronous muscles, such as the sound-producing muscles of rattlesnakes, fish and many insects, are characterized by hypertophy of the sarcoplasmic reticulum and a reduction in the diameter of the myofibrils; features that reduce the diffusion distance, and therefore diffusion time, for Ca^{2+} into and out of myofibrils (Fawcett and Revel, 1961; Josephson and Young, 1987; Schaeffer et al., 1996; Lindstedt et al., 1998). Increasing the volume and hence the surface area of the sarcoplasmic reticulum increases its capacity to take up Ca^{2+}, and thus increases the rapidity with which the muscle can be turned off to end contraction. In addition to the ultrastructural modifications, there are also biochemical changes associated with the capacity for high-frequency operation of synchronous muscles, including reduced Ca^{2+} affinity of the control proteins, a feature that facilitates dissociation of Ca^{2+} and its removal from the myofibrils, and enhanced association and dissociation rates of cross-bridges, with a related increase in the shortening velocity of the muscle and therefore the distance of shortening achieved during a brief contraction (Rome et al., 1996, 1999).

Asynchronous muscles, like synchronous ones, are activated by motor neuron action potentials and the resulting muscle fiber depolarization; but an asynchronous muscle, when turned on, can contract in an oscillatory fashion if it is attached to an appropriate, resonant load (for reviews of asynchronous muscle and references, see Tregear, 1975; Pringle, 1978; Dudley, 2000; Josephson et al., 2000). The contraction frequency of an oscillating, asynchronous muscle is the resonant frequency of the load, and not that of the motor neuron impulses that activate the muscle. The time course of neurally evoked activation is slow in those asynchronous muscles that have been examined, and only low-frequency neuronal input is needed to maintain full activation. During normal operation, there are typically 3–10 oscillatory contraction cycles for each muscle action potential. The features of asynchronous muscles that allow oscillatory contraction are delayed muscle activation following stretch and delayed deactivation following shortening. It is mechanically linked activation and deactivation, coupled with mechanical resonance, that determines the time course of contraction rather than neurally controlled activation and deactivation. The asynchronous mode of operation bypasses the necessity for rapid Ca^{2+} release and rebinding that is inherent to synchronous muscles if they are to be fast. The wing-stroke frequencies of insects that use asynchronous flight muscles have been found to be correlated with the time constants of the activation and deactivation processes of the flight muscles (Molloy et al., 1987). Presumably, the rate constants of the activation and deactivation processes determine the range of frequencies over which an asynchronous muscle can operate.

Fast, synchronous muscles occur widely in the animal kingdom; asynchronous muscles are known to occur only in insects. Asynchronous muscles power flight in many insects and sound production in a few. The distribution of asynchronous muscles in different insect groups suggests that the asynchronous mode of operation has arisen independently at least 7–10 times (Cullen, 1974; Pringle, 1981; Dudley, 2000). Asynchronous flight muscle is characteristic of some of the more speciose taxa, including Coleoptera, Diptera and Hymenoptera. Dudley (1991) estimates that approximately 75 % of the insect species that fly do so with asynchronous muscle.

Although there are exceptions, asynchronous flight muscles are generally associated with high wing-stroke frequencies. It has been suggested that asynchronous muscles have been evolutionarily favored in many insect groups because they are more powerful and more efficient during high-frequency operation than are synchronous muscles (Josephson and Young, 1981; Lindstedt et al., 1998; Dudley, 2000). Asynchronous muscles are likely to be more powerful than synchronous ones because they do not have to invest heavily in sarcoplasmic reticulum to achieve high operating frequencies. The reduction in the volume of sarcoplasmic reticulum increases the space in a given mass of muscle for myofibrils. Asynchronous muscles are likely to be more efficient than synchronous ones because they do not have to cycle Ca^{2+}, and incur the rather high Ca^{2+}-cycling costs, on each contraction.

Although the mass-specific power output from asynchronous muscles is predicted to be greater than that of fast, synchronous ones, there is actually little direct evidence supporting this expectation. The few values for maximum power output that have been measured directly from living insect muscle with the work-loop approach are not obviously different for asynchronous and synchronous flight muscles. The maximum power outputs recorded from asynchronous flight muscles of a beetle (*Oryctes rhinoceros*) and a bumblebee (*Bombus terrestris*) were 30 W kg^{-1} and 60 W kg^{-1}, respectively, in the classic study of Machin and Pringle (1959). In a more recent examination of bumblebee muscle, the maximum power output averaged 45 W kg^{-1}, but ranged up to slightly more than 100 W kg^{-1} in particularly strong preparations (Josephson, 1997b). Equivalent values for synchronous flight muscles of insects are: katydid (*Neoconocephalus triops*), 76 W kg^{-1} (Josephson, 1985); locust (*Schistocerca nitens*, *S. americana*), 73 W kg^{-1} (Mizisin and Josephson, 1987), 68 W kg^{-1} (Malamud et al., 1988); sphinx moth (*Manduca sexta*), 90 W kg^{-1} (Stevenson and

Josephson, 1990). Marden (1987) measured the lifting capacity during takeoff from a large number of insects to determine the maximum power output of the flight musculature. In neither Marden's analysis, nor in that of Ellington (1991), who used Marden's data and a different aerodynamic model to calculate power output, was there any obvious difference in mass-specific power output of flight muscle between animals using synchronous flight muscles and those with asynchronous muscles. Further, in Marden's (1987) data, the ratio of flight muscle mass to body mass was similar in bees, wasps and beetles, which use asynchronous muscles, and in sphinx moths, which use synchronous muscles. If asynchronous muscles were more powerful, one might expect that the power necessary for flight would be obtained with a relatively smaller muscle volume in animals with asynchronous muscles than in those with synchronous ones.

Measured values of power output from bumblebee muscles (Josephson, 1997b) were disturbingly variable from preparation to preparation. The problem here was probably one of muscle geometry. Living insect muscles are very sensitive to anoxia and perform well only if the tracheal system, which is the route of oxygen supply, is intact. Whole muscles, with an intact tracheal supply, perform much better than do parts of muscles or fiber bundles in which the tracheation is necessarily disrupted. There are just four power muscles in the bumblebee flight system, a dorso-ventral pair and a longitudinal pair. Each of the muscles is rather stout. The dorso-ventral muscle, which was the one examined by Josephson (1997b), runs from the cuticle of the dorsal tergum to that of the ventral sternum. Mechanical recordings were made by surgically isolating the cuticle at the dorsal attachment of the muscle from the surrounding exoskeleton, and then fixing the isolated patch of cuticle with its connected muscle to a force transducer. Because the muscle has a broad origin and insertion, it proved difficult to isolate one end of the muscle and arrange it for mechanical recording such that the patches of cuticle at the muscle's origin and insertion were in precisely the same relationship to one another as in the intact animal. Only if the muscle origin and insertion are in the same relative position as in the intact animal will the lengths of all the fibers in the muscle be similar to their normal *in vivo* lengths. Further, the relatively large cross-sectional area of the muscle increases the difficulty of imposing length changes on the muscle as a whole that will result in muscle strain in the individual fibers throughout the muscle similar to those that might be experienced in the intact organism. And power output in the bumblebee muscles is extremely sensitive to changes in muscle length or strain. Changing the muscle length by only 1 % from its optimal value, or changing the strain by 1.2 % of the muscle length from its optimal value, each reduced power output by 50 % (Josephson, 1997a). The variability in measured values of maximum power output from the bumblebee muscle probably reflects varying success in mounting the muscle such that the lengths of the fibers in the muscle and the strain that they experienced during imposed sinusoidal length change were both similar to those of the muscle fibers *in vivo*.

Achieving appropriate loading and stretch of all the fibers of a muscle during work measurements was recognized as a problem by Darwin and Pringle (1959) and Machin and Pringle (1959), who also, by introducing the beetle basalar muscle as a preparation, provided a solution to the problem. The basalar muscle of beetles is an asynchronous, direct flight muscle. It inserts dorsally on a cuticular cap. The force applied to the cap is transmitted through a short apodeme to the basalar sclerite of the wings. Length changes and loads applied to the apodeme are automatically distributed to the fibers of the basalar muscle just as in an intact insect. Using the apodeme as an attachment point for mechanical recordings rather than a broad patch of cuticle should greatly reduce inequalities in stress and strain among the different fibers of a muscle.

Shortly after the introduction of the beetle basalar muscle as a physiological preparation, the focus in studies of asynchronous muscle shifted to glycerinated or detergent-extracted fibers rather than live muscles, and only a handful of studies since have considered living, asynchronous muscle. Glycerinated and detergent-extracted fibers offer several advantages over living muscles for functional studies. They may be stored for reasonably long times, freeing investigators from some of the problems involved in collecting and maintaining living insects. Most importantly, glycerinated or detergent-extracted fibers allow better control over the chemical environment in which the contractile material operates than is possible with living muscle. Unfortunately, the mechanical power output obtained from glycerinated fibers has been low, probably because of limitations in the rate at which the working crossbridges can be supplied with ATP by diffusion from a bathing solution. Only in the recent work of Gilmour and Ellington (1993a,b) has the mechanical power obtained from glycerinated fibers of asynchronous muscle approached that expected from the muscle performance in living insects.

In the following study, we used the basalar muscle of a beetle (*Cotinus mutabilis*) to examine power output by a living, asynchronous muscle. As had been hoped, the beetle muscle proved to be a much more consistent preparation than had been the dorso-ventral muscle of bumblebees. The maximum power output obtained from the beetle muscle was substantially greater than any yet recorded with similar approaches from synchronous flight muscles of insects, supporting the hypothesis that asynchronous flight muscles have been evolutionarily favored because they have greater power output. Since there is little published information on beetle flight muscle, we also describe the organization of the beetle basalar muscle, its activation and performance during tethered flight, and its basic physiology, We consider in some detail the factors that determine mechanical power output from the muscle during oscillatory contraction.

Materials and methods

Animals

The muscles studied were from *Cotinus mutabilis* (Gory and Percheron), a scarab beetle. The beetles were captured in

Irvine, CA, USA and were raised in our laboratory following procedures developed by C. Conlan of the Mycogen Corporation, San Diego, CA, USA. Adults were housed in a flight cage and fed pieces of apple. Eggs were collected in pots of soil, and larvae were raised in and fed on the depleted medium left after harvesting mushrooms by a commercial mushroom farm. Adult beetles usually weighed between 1 and 1.5 g.

Muscles

All measurements were from the metathoracic basalar muscle, which is a depressor of the hindwing. Useful descriptions of the anatomy of beetle flight muscles are provided by Stellwaag (1914), Korschelt (1923) and Darwin and Pringle (1959).

Correlating wing strokes and electromyographic activity

Muscle action potentials during tethered flight were recorded from a pair of silver wires implanted into the ventral origin of the basalar muscle through small holes drilled in the sternum. The electrode wires were 100 μm in diameter and were insulated to the tip. Before implanting the electrodes, the end of each wire was held at the edge of a flame until the silver at the tip melted and formed a small bead. The size of the holes made in the exoskeleton matched the size of the bead, so that once a wire was inserted through the exoskeleton it could not be easily retracted. Each wire was fixed with low-melting-point wax to the sternum and then dorsally to the pronotal shield before being connected to an a.c.-coupled differential amplifier. The signals were amplified (×100, band pass 30 Hz to 10 kHz) and passed to an analog/digital converter and a computer for display and storage. When the electrodes were in place, the pronotal shield of the beetle was fixed with wax to a spring-steel beam. Force transducers on the beam measured the deflection of the beam resulting from thrust developed by the wings during flight. Between bouts of flight, the beetle was given a small stryofoam ball which it held with its legs. Flight was initiated by removing the styrofoam ball and blowing an air stream over the animal.

Wing-beat frequency and temperature in free flight

An animal was induced to fly by repeatedly throwing it into the air in a flight chamber of dimensions 51 cm×54 cm×70 cm (depth×width×height). The wing-stroke frequency during flight was measured either using an optical tachometer (Unwin and Ellington, 1979) or by recording the flight tone with a microphone held beneath the animal while it was flying or hovering. Signals were recorded with a tape recorder for later analysis. After several recordings of flight frequency had been obtained, the animal was caught in a hand enclosed in a cotton glove. A thermocouple probe, 0.5 mm in diameter, was quickly inserted into the thoracic musculature on one side, and the thoracic temperature was recorded. The wing-stroke recordings were processed with an analog/digital converter and displayed on a computer. Wing-stroke frequency was determined from segments of these recordings that were 5–10 cycles long. Five determinations, each from a different segment, were made from each preparation and averaged. Work output at the muscle temperature and wing-stroke frequency of flight was then measured from the basalar muscle of the animal, using the muscle on the side opposite to that impaled to determine thoracic temperature. The delay between the measurement of flight frequency and that of work output by the flight muscle, i.e. the time required to prepare the muscle for mechanical recording and actually make the work measurements, was 1.5–2 h.

Measuring muscle force

A beetle was immobilized by chilling, and its wings and legs were removed. The sternum of the prothoracic segment was removed to expose the prothoracic ganglion and the anterior part of the fused meso-metathoracic ganglion. The anterior and posterior connectives and the lateral nerves from the thoracic ganglia were sectioned, and the ganglia were removed. In all but a few experiments, the muscle was activated using stimulating electrodes implanted in the ventral origin of the muscle. The electrodes, silver wires 100 μm in diameter, were inserted through small holes made in the exoskeleton and waxed in place. In some early experiments, a widely spaced, triangular array of stimulating electrodes was used, with one electrode wire serving as a current source and the other two as current sinks, or with two current sources and one sink. The maximum tetanic force initiated by stimulation with three-electrode arrays was no greater than that obtained with two widely spaced electrodes in the muscle, and all the experiments to be reported in which the muscle was stimulated with implanted electrodes used a pair of wires for stimulation. The preparations that did not have implanted stimulating electrodes were some of those used in analyzing the innervation pattern of the muscle, in which the muscle was stimulated by a suction electrode on the motor nerve rather than directly with implanted wires. When the stimulating wires were in place, the beetle was fixed, dorsal side up, to a thin plastic plate using rapidly hardening epoxy cement. The beetle was set in the epoxy such that the long axis of the basalar muscle was vertical in the roll plane. After the epoxy had hardened, the apodeme at the insertion of the muscle and an attached piece of distal cuticle were exposed by removing the surrounding structures. The preparation was then transferred to a platform on the shaft of an ergometer (a device for subjecting the muscle to controlled length changes). The preparation was fixed to the platform with double-sided tape. A thermocouple probe mounted in a 21 gauge hypodermic needle (0.81 mm outside diameter) was inserted through the tergum into the thorax on the side contralateral to the experimental muscle. The thermocouple monitored thoracic temperature. The shaft of the ergometer was vertical. The platform at the end of the ergometer shaft was obliquely positioned on the shaft in what would be, when the animal was mounted, the anterior–posterior axis. When the beetle was properly positioned on the platform, the muscle was vertical, with its major axis in line with the ergometer shaft. When the animal was in place, the apodeme of the muscle was slipped into a

hook projecting from a force transducer. The force transducer was mounted in a manipulator, which allowed positioning of the muscle apodeme so that the exposed distal parts of the muscle were oriented normally with respect to adjacent structures. The muscle was oriented properly, stretched until it was just taut, and then the apodeme was fixed firmly into the hook on the transducer with a small dab of melted wax.

The ergometer was constructed around a B&K 4810 shaker. A slotted vane on the shaker shaft was positioned so that it interrupted a light beam between a light-emitting diode and a United Detector Technology PIN SL5 position-sensing photodiode. The output of the photodiode monitored the position of the shaft and provided the feedback signal for the electronic servo-system that controlled the movement of the shaft. Command signals determining the position of the ergometer were generated by a computer using the program LabVIEW (National Instruments Co., Austin, TX, USA).

The force transducer was made from a short blade of spring steel mounted in a steel rod. The dimensions of the segment of the blade that protruded from the rod were 7.2 mm×4.0 mm×0.38 mm (length×width×height). Displacement of the blade was monitored with a pair of semiconductor strain gauges fixed on the top and bottom faces of the blade near its base. The hook used to attach the transducer to the muscle was fashioned from an insect pin and was attached to the blade, perpendicular to the long axis of the blade, near its free end. The stiffness of the transducer was $40\,\mu m\,N^{-1}$ and the resonant frequency approximately 2.5 kHz. The transducer compliance would allow the muscle to shorten during an isometric, tetanic contraction (force developed 0.1–0.3 N) by less than 0.2 %. Because there is some bending of the transducer, the length change experienced by the muscle during imposed strain was somewhat less than the measured displacement of the ergometer shaft. Forces as large as 1.5 N were developed during large-amplitude, oscillatory strain, which would result in transducer bending, and overestimate of the muscle strain, by less than 1 % of the muscle length.

During experiments, the muscle was stimulated with 1 ms shocks presented singly or in tetanic bursts at 100–200 Hz. The exposed portion of the muscle was moistened periodically with locust saline (Usherwood, 1968; pH adjusted to 6.8 at room temperature with NaOH or HCl). Muscle temperature was maintained at a selected value with a feedback system that controlled the intensity of the beam from a microscope lamp that shone on the thorax.

At the end of an experiment, the muscle was superfused with 70 % ethanol while still attached to the force transducer. The muscle was fixed *in situ* for approximately 30 min before being detached from the force transducer. The preparation was then removed from the ergometer and stored in 70 % ethanol. After one to several weeks of fixation, the thorax was hemisected, and overlying tissue was removed to expose the medial surface of the experimental muscle. The length of the muscle along its medial surface, which is where the longest fibers occur, was measured with an ocular micrometer. The experimental muscle was then removed and stored in 70 % ethanol. Later, usually within a few days, the muscle was rehydrated overnight in saline and weighed. Ten basalar muscles were weighed when fresh and then reweighed after alcohol fixation for several days followed by rehydration. The muscles lost weight during fixation and rehydration. The mean ratio of original muscle mass to rehydrated mass was 1.17±0.0797 (mean ± S.D., N=10). Therefore, the masses of all rehydrated experimental muscles were multiplied by 1.177 to obtain an estimate of their original wet mass. Four alcohol-fixed muscles were teased into individual fibers, whose lengths were measured. The mean fiber length of these muscles averaged 88±1.4 % (mean ± S.D.) of the muscle length along its medial surface (see below). Therefore, the average length of fibers within a muscle was obtained by multiplying the muscle length as measured along its medial surface by 0.88. Muscle cross-sectional area (cm^2) was obtained by dividing the corrected muscle mass (g) by the average fiber length (cm), a procedure that assumes that the muscle density is $1\,g\,cm^{-3}$.

Measuring work and power

Mechanical work output by the muscle was determined using the work-loop approach. The muscle was stimulated tetanically and, during the plateau of the tetanus, subjected to a series of sinusoidal length changes. The work output of a selected cycle was measured as the integral of $F\mathrm{d}L$ evaluated over a full cycle, where F is muscle force and L is muscle length. Further details of the methods used to characterize muscle work output are described where relevant in the text.

Results

Muscle structure

The masses of muscles used in experiments were measured after alcohol fixation, dissection and rehydration. The mean mass of the basalar muscle, corrected for the expected shrinkage during fixation, was 41.2±7.2 mg (mean ± S.D., N=105). The masses of the animals from which these muscles came averaged 1.28±0.26 g (mean ± S.D., N=105).

The basalar muscle is one of the set of asynchronous muscles in the thorax that power flight; the other asynchronous muscles are the subalar, the dorsal longitudinal, the dorsal oblique, the anterior dorso-ventral and the posterior dorso-ventral. The total mass of the asynchronous muscles was determined by removing, rehydrating and weighing all the asynchronous muscles from one side of the thorax in animals fixed in 70 % ethanol. The asynchronous muscles were distinguished from the other thoracic muscles, some of which are control muscles for flight, by their fibrillar structure and pink color. The pink color of the fibrillar muscles presumably reflects a high concentration of mitochondria. The non-fibrillar muscles were, in comparison, light tan to white. The measured mass of the asynchronous muscles in a hemithorax was corrected for the expected shrinkage during fixation and multiplied by 2 to obtain the total mass of the asynchronous muscles in the whole thorax. The mean mass of the asynchronous muscles in a beetle was 241±39 mg (mean ± S.D.,

N=8). The asynchronous muscles together made up 19.3±1.8 % (mean ± S.D.) of the total body mass of these animals, which had been weighed before fixation. The right and left basalar muscles, with a combined mass of approximately 83 mg, together represent by mass approximately one-third of the power muscles of flight.

The basalar muscle is a parallel-fibered muscle whose fibers run basically in a dorso-ventral direction. The sternum, on which the fibers originate, curves upwards laterally, with the result that not all the fibers of the muscle are the same length. The fibers are longest at the medial face of the muscle and shortest at the lateral edge. The distribution of fiber lengths in the muscle was measured to determine the mean fiber length so that muscle strain during length changes imposed upon the muscle might be properly evaluated. Basalar muscles from four animals were teased apart into individual fibers whose lengths were measured with an ocular micrometer. The muscles analyzed were composed of 84–94 fibers whose measured lengths ranged from less than 4 to more than 7 mm (Fig. 1). We measured the lengths of muscles used in experiments along the medial surface, which is where the fibers are longest. In the four muscles of Fig. 1, the ratio of the mean fiber length to the muscle length measured along the medial surface was 88.2±1.4 % (mean ± S.D.). Thus, the muscle length measured along the medial surface overestimates the mean fiber length in the muscle, and underestimates the mean strain experienced by all fibers, by approximately 13 %. The muscle length used in calculations of muscle cross-sectional area and strain are based on the mean fiber length, determined by multiplying the measured length of the muscle along its medial surface by 0.88.

Basic muscle physiology

Motor unit composition of the muscle

Information on the number of motor units making up the basalar muscle was obtained by stimulating the muscle with shocks of varied intensity so as to activate differing numbers of motor units. A sudden jump in the amplitude of evoked twitches during a series of trials in which stimulus intensity was gradually increased was taken as indicating that a new motor unit had been activated; a sudden drop in twitch amplitude during a series with decreasing stimulus intensity was interpreted as indicating that the stimulus had dropped below the threshold of a previously participating unit. The stimuli were 0.2 or 1 ms voltage pulses, delivered to the muscle through implanted wire electrodes or, in some preparations, through a suction electrode on the motor nerve to the muscle. The intertrial interval ranged from 30 to 120 s in different experiments. Stimulating the basalar nerve directly lessened the possibility that the recorded responses were due in part to contraction of neighboring muscles activated by volume conduction from the implanted electrode wires, rather than responses of the basalar itself. However, the extensive dissection required to expose the basalar nerve, which destroyed some of the tracheal air supply to the muscle and

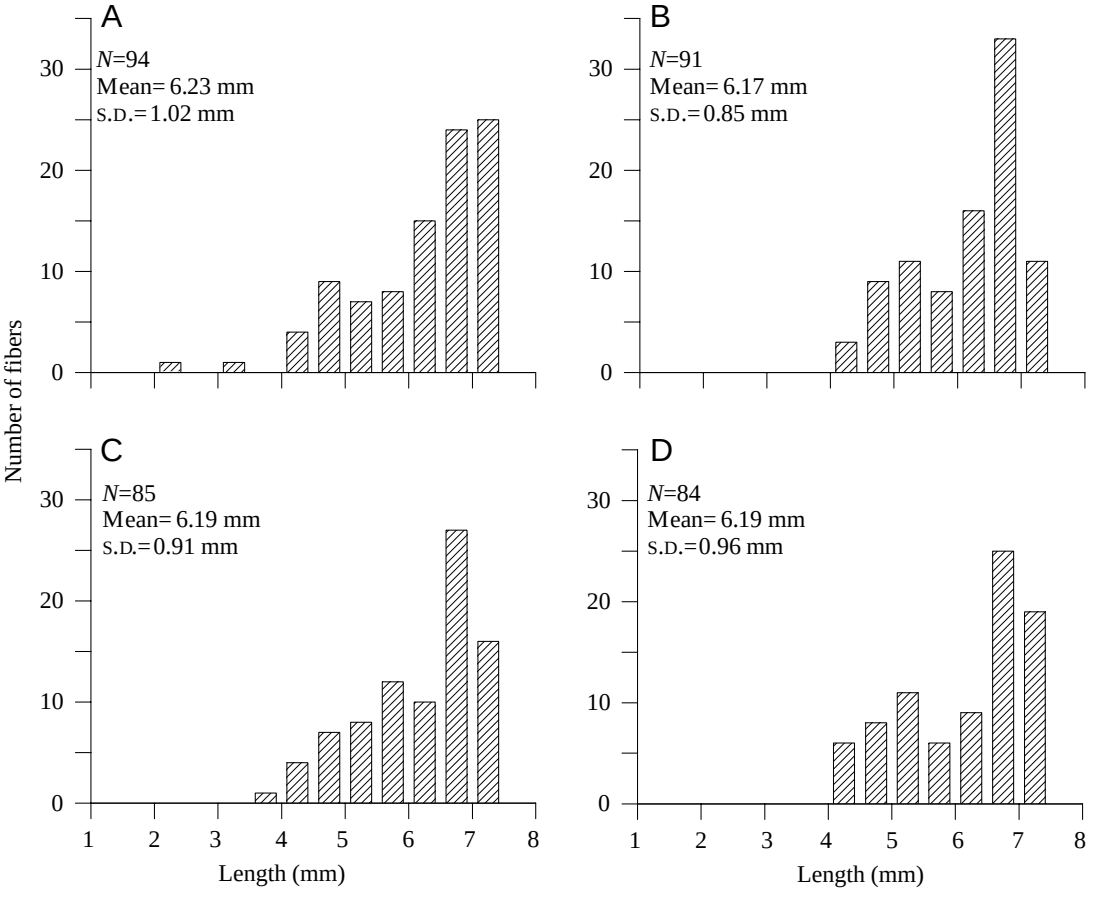

Fig. 1. Fiber length distribution in basalar muscles of four beetles.

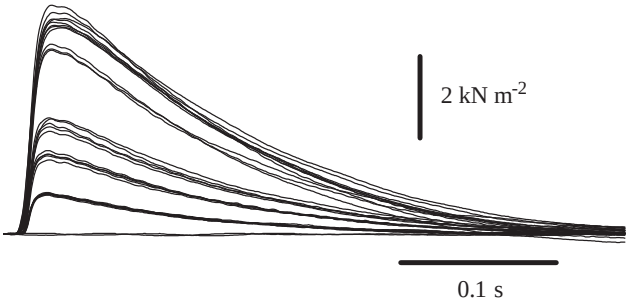

Fig. 2. Isometric twitches in response to repeated stimuli of progressively decreasing amplitude at 30 °C. The presence of five more-or-less discrete force levels indicates that the muscle is composed of at least five motor units.

probably also interfered with the circulation of hemolymph to the muscle, apparently diminished muscle performance, and twitch forces were smaller when using nerve stimulation than with direct stimulation through implanted wires. It should be noted that 'direct' stimulation of an insect muscle actually activates fibers of the muscle indirectly, by exciting the motor neuron processes that course through the muscle, and motor units appear and disappear in an all-or-nothing fashion with changes in stimulus strength when using direct muscle stimulation just as they do with nerve stimulation (see, for example, Josephson, 1973).

Up to five excitatory motor units were identifiable on the basis of changing twitch amplitude with changing stimulus intensity when using either nerve stimulation or direct stimulation. Of the eight preparations in which the muscle was stimulated directly, four had five identifiable excitatory motor units, three had four excitatory units, and one had three detectable motor units. An example of the results from a preparation with five discernible excitatory motor units is shown in Fig. 2. Of the five preparations in which nerve stimulation was used, one was found to have five excitatory motor units, one had four, two had three and one had two motor units. Evidence for inhibitory innervation to the basalar muscle was found in the experiments with nerve stimulation. In five of the six preparations with nerve stimulation, in all of which the stimuli used were of progressively decreasing strength, reducing the stimulus intensity in some part of the effective range resulted in an increase rather than a decrease in twitch amplitude. The increase in twitch size with decreasing stimulus intensity suggests that the stimulus had dropped below the threshold of an inhibitory axon. The increase in twitch force associated with the dropping out of the inhibitor was approximately 20 % (21.9±3.8 %, mean ± S.D.) in the three preparations with nerve stimulation in which twitch traces were stored for later analysis. There was no evidence in these experiments for inhibitory axons when using direct muscle stimulation, although in other experiments with direct stimulation we have seen several instances of a decrease in contractile force with increasing stimulus intensity, suggesting the activation of an inhibitory axon.

The approach used above to determine the motor unit composition of the basalar muscle gives a minimum estimate of the number of motor units in the muscle. Units that produced a very small twitch force would not be detected. Two or more units that had very similar thresholds might easily be counted as a single one. Our conclusion is that there are at least five excitatory motor axons to the basalar muscle and at least one inhibitor. These results are in broad agreement with those of Darwin and Pringle (1959), who reported 7–9 axons, presumably motor axons, in the basalar nerve of two beetle species, and with the results of Ikeda and Boettiger (1965b) who, in a detailed electrophysiological study, found eight excitatory and at least one inhibitory axon innervating the basalar muscle of a rhinoceros beetle (*Oryctes rhinoceros*).

Twitch and tetanic tension

The length of the muscle was adjusted to approximate the normal *in vivo* length as judged by the positions of the cuticular cap and apodeme of the muscle relative to surrounding structures. Twitch and tetanic responses were initiated using stimuli that were strong enough to evoke maximal contractions. The stimulation frequency for tetanic contractions was 100 Hz at 30 °C and 150–200 Hz at higher temperatures. As seems to be characteristic of asynchronous muscles, active force (the increase in force above passive level upon stimulation) is low and twitches are slow (Fig. 3; Table 1; for examples of twitch and tetanic force from other asynchronous muscles, see Machin and Pringle, 1959; Ikeda and Boettiger, 1965a; Josephson and Young, 1981; Josephson and Ellington, 1997). A temperature change from 30 to 40 °C, which is over the range at which the muscle normally operates, had surprisingly little effect on muscle contraction kinetics (Fig. 3B; Table 1). Twitch rise time shortened slightly, but not significantly ($P>0.3$, two-tailed *t*-test on paired samples), with the 10 °C increase in temperature, twitch relaxation time decreased proportionally slightly more ($P<0.02$), and there was essentially no change in the maximum tetanic tension. In this set of experiments, the maximum tetanic stress averaged slightly less than 20 kN m^{-2} at both 30 and 40 °C. The measured tetanic stress was approximately twice as great in another set of experiments in which tetanic force was measured at 35 °C and at the muscle length that was optimal for work output (see Fig. 18). Why there was a large difference in

Table 1. *Some features of isometric twitches and tetanic contractions from the beetle basalar muscle*

	30 °C	40 °C	Q_{10}
Twitch			
Tension (kN m^{-2})	4.2±1.9	2.9±1.2	0.7±0.1
Rise time (ms)	20.1±4.3	17.4±4.1	1.2±0.4
Time from peak to 50 % relaxation (ms)	105±14	68±21	1.7±0.6
Tetanic tension (kN m^{-2})	19.1±8.0	19.2±4.5	1.1±0.4
Twitch tension/tetanic tension	0.19±0.05	0.14±0.06	0.7±0.1

Values are shown as means ± S.D., N=7.

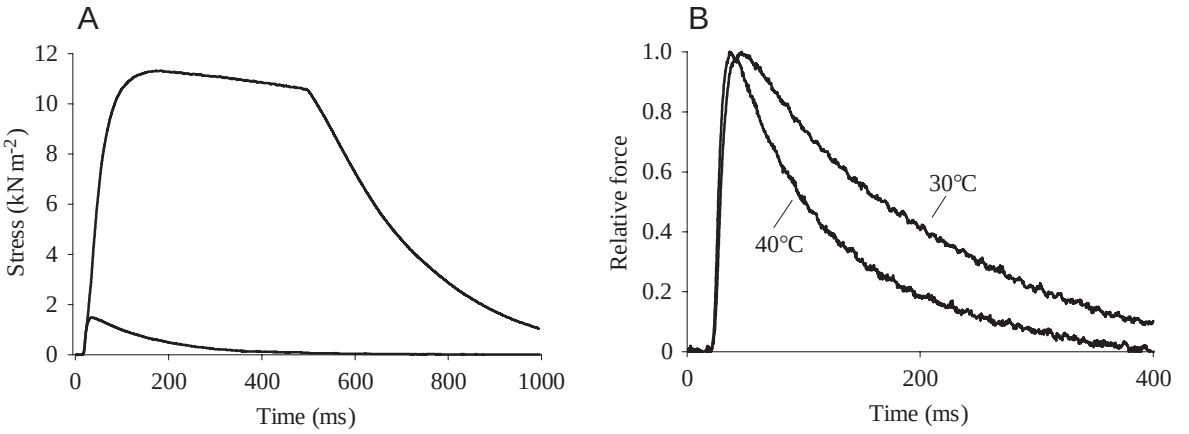

Fig. 3. (A) A twitch and a tetanic contraction from a basalar muscle at 35 °C; tetanic stimulation frequency 150 Hz. (B) Twitches from a different basalar muscle at 30 °C and 40 °C.

the measured stress between these two sets of measurements is not known.

Force and work at different muscle lengths

A muscle was stretched in a series of steps, beginning at a length short enough that there was little or no active or passive force. The individual length steps were 0.064 mm (approximately 1 % of muscle length). The muscle was left at each step length for 2 min. One minute after each stretch, the muscle was stimulated with a single stimulus to produce a twitch. Two minutes after the stretch, just before the next stretch, the muscle was stimulated with a tetanic burst at 120 Hz to initiate an isometric tetanus. The twitch and tetanic stimuli were adequate to produce maximal mechanical responses. During the plateau of the tetanic contraction, the muscle was subjected to a short burst of sinusoidal strain at 60 Hz with predicted peak-to-peak amplitude of 2.5–3 % (the actual strain depended on the *in vivo* muscle length, information about which was not available until after the end of the experiment). The sequence of stretch, twitch stimulation, tetanic stimulation and sinusoidal strain was continued as the active tetanic force rose to a maximum and began to decline. When the active tetanic force had declined to approximately 80 % of its maximum, stretching was ended and the muscle was instead shortened in a series of steps, each approximately 2 % of the *in vivo* length, and subjected to the same regime of twitch stimulation, tetanic stimulation and imposed cyclic strain as during the increasing length series. The muscle temperature was maintained at 35 °C throughout these experiments. The work done during the imposed cyclic strain was taken as the mean area of the work loops for cycles 2, 5 and 8 of each series. The strain amplitude used, 2.5–3 %, was well below that

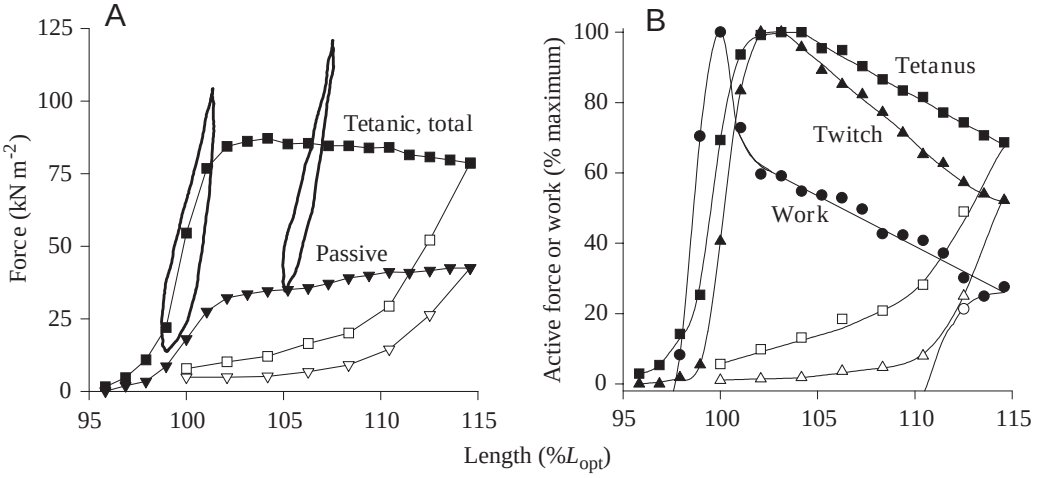

Fig. 4. Isometric force and net work at different muscle lengths during progressive muscle stretch and release. (A) Passive force and peak tetanic force (passive force plus active force). Filled symbols were obtained at progressively longer lengths during stretch, open symbols at progressively shorter lengths during the subsequent release. Two work loops, obtained with 2.8 % peak-to-peak strain, are shown. The left-hand work loop centers at the optimal muscle length, L_{opt}, for work output. (B) Active force (the increase in force above passive level) during twitch and tetanic contractions and net work per cycle at different muscle lengths. Filled symbols were obtained during stretch, open symbols during subsequent release. The continuous curves in A and B are fitted by eye. The trajectory of the work curve through the *x* axis is based on negative work values obtained at short lengths during stretch and release.

optimal for work output (approximately 5.4 % at 60 Hz and 35 °C; see Fig. 10). Using a relatively small strain meant that the work output could be more accurately associated with a particular muscle length than would be true with a larger strain, one perhaps closer to the optimum and giving greater work output, but during which the muscle length would cover a greater span.

The five replicate experiments in this series all gave results similar to those illustrated in Fig. 4. The principal conclusions that we draw from these experiments are the following.

(i) Passive force during lengthening rises to a yield point, beyond which it continues to rise but at a much reduced slope (Fig. 4A). A similar yield during low-frequency stretch of passive muscle has been found in asynchronous flight muscle of the bug *Lethocerus* (White, 1983; Granzier and Wang, 1993a,b) and a bumblebee *Bombus terrestris* (Josephson and Ellington, 1997), and may be a common feature of asynchronous muscles. In synchronous muscle, force yield during stretch is commonly seen in stimulated muscle (for a review, see Josephson and Stokes, 1999), but does not seem to be a property of passive muscle (Granzier and Wang, 1993b).

(ii) The effects of stretch are not reversible, at least not for stretches of the trajectory and time course used in these experiments. The muscle showed marked hysteresis during a stretch/release cycle. Passive force, active force and work were all much less for the measurements made during the progressive release following lengthening (open symbols in Fig. 4) than they were at the same muscle lengths during the preceding stretch series. Similar hysteresis has been described in other muscles, including asynchronous flight muscle from the bug *Lethocerus* and mammalian cardiac muscle (White, 1983; Granzier and Wang, 1993a; Granzier and Irving, 1995), where it has been ascribed to the unfolding of titin or minititin molecules during stretch (Granzier and Wang, 1993a; Helmes et al., 1999). Some of the hysteresis during a long, slow lengthening–shortening cycle of the beetle muscle may be due to length-dependent unfolding of titin or other large molecules, but some of the hysteresis is due to time-dependent processes, as is evident from the slow decline in tension (=stress relaxation) seen after rapid stretch when the muscle is held at the stretched length (Fig. 5). Stress relaxation of stretched, unstimulated muscle, similar to that in the beetle muscle, has been described for frog (*Rana esculenta*, *R. temporaria*) muscle fibers (Buchthal et al., 1951), for the synchronous flight muscle of a locust (*Schistocerca americana*) (Malamud, 1989) and for the asynchronous flight muscle of a bumblebee (Josephson and Ellington, 1997). An important consequence of stress-relaxation is that muscle force during progressive lengthening, and the amplitude and shape of a length/tension curve based on measurements of muscle force, vary with the time after stretch at which the measurements are made.

C-filaments, composed of minititin, connect the ends of the thick filaments to the Z-disks of asynchronous muscles and are major contributors to the passive tension in a muscle when it is stretched (Granzier and Wang, 1993a,b). It is easy to see how non-reversible or slowly reversible unfolding of C-filaments during stretch might increase the filament compliance and lead to a substantial drop in passive tension during subsequent muscle shortening, but it is less obvious why lengthening of elements lying effectively in parallel with the thin filaments should result in a marked reduction in active tension at subsequently shortened lengths. If the C-filaments were in series with the sarcomeres, it could be proposed that their stretching allowed the sarcomeres to shorten to less favorable lengths for force production; but they are not. The depressed active force seen in the beetle muscle during the progressive shortening following stretch is consistent with the proposal of Granzier and Wang (1993a) that the amplitude of the active force produced when an asynchronous muscle is stimulated is dependent upon the passive force at the time of stimulation, and a reduction in the passive force because of C-filament unfolding leads to an associated reduction in active force.

(iii) The optimal muscle length for work output was shorter than that for isometric force (Fig. 4B). The optimal muscle length for twitch force was 2.0±0.3 % (mean ± S.E.M., N=5) greater than that for work per cycle. The optimal length for tetanic force was difficult to determine precisely because of the asymmetrical shape and broad plateau of the relationship

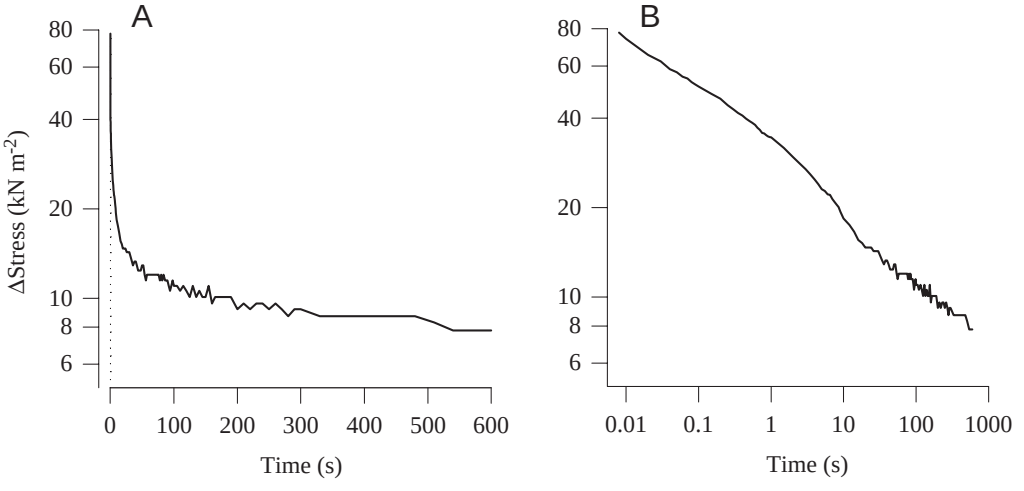

Fig. 5. Stress relaxation of the beetle basalar muscle. The muscle was rapidly stretched (7.6 % in 13 ms) from an initial length approximating the normal *in vivo* length. The force plotted in A and B is the increase above the pre-stretch level. (A) The log-transformed value of the force increase is not a linear function of time, indicating that force decay is not an exponential process. (B) The same data as in A plotted on log–log coordinates. Force decay continues, albeit at an ever-decreasing rate, for many minutes.

between tetanic force and muscle length; however, from inspection, it was obvious that the optimal length for tetanic force was at least as long as that for twitch force.

(iv) The length/work curves in this series were significantly narrower than the length/tension curves for twitches, which were in turn narrower than the length/tension curves for tetanic contractions. The width of the curve relating work output and muscle length, measured at 80 % of the maximum value, was 2.2±0.6 % of the optimal length (mean ± S.D., mean span was from −0.9 % of the optimal length to 1.3 %, *N*=5). The width at 80 % for the twitch force curve was 7.4±5.6 % of the optimal length for work output (mean ± S.D., mean span 0.6–8.0 %) and that for the tetanic force curve was 14.2±3.9 % (mean ± S.D., mean span 0.2–34.6 %).

(v) Work loops coursed in a 'northeast' to 'southwest' direction and crossed the length/tension curve for total tetanic force such that the maximum force reached during the cyclic strain of a work loop was greater than that of an isometric contraction at the maximum length reached in the loop. The position of the work loops with respect to the isometric length/tension curve was similar to that found recently for the asynchronous flight muscle of a bumblebee (Josephson, 1997a) and different from that in early reports of Boettiger (1957, 1960) and Machin and Pringle (1959), who describe work loops in asynchronous bumblebee and beetle muscles as lying entirely below the active length/tension curve or as crossing the length/tension curve but being rotated clockwise with respect to it so that the peak force in the work loop was less than that at the equivalent length in an isometric contraction.

Stretch activation and shortening deactivation

The features of asynchronous muscle that can lead to oscillatory contraction when a muscle is attached to an appropriate mechanically resonant load are delayed activation following stretch and delayed deactivation following shortening (see discussion in Josephson et al., 2000). Examples of stretch activation and shortening deactivation are shown in Fig. 6. In the experiments of this series, a muscle was stretched for a short distance at constant velocity and, after a delay, released at constant velocity. The stretch and release velocities ranged up to 75 mm s^{-1}. In an unstimulated muscle, the force rose during stretch but then began to decline immediately at the end of stretch (Fig. 6A,C). This is the behavior expected for a passive visco-elastic structure. In a stimulated muscle, in contrast, force rose during the stretch but, at least with moderately fast stretches, continued to rise at the end of stretch to a maximum reached well after the end of lengthening. For example, in the more rapid stretch of the two illustrated in Fig. 6C, the force in the stimulated muscle reached a maximum (marked by the arrow) approximately 8 ms after the end of stretch. The increase in force following the end of lengthening is a manifestation of delayed stretch activation. With the slower stretch in Fig. 6C, some of the activation occurred during the course of the stretch, and the post-stretch rise in force, while present, is less conspicuous than that with the faster stretch. The converse of stretch activation is shortening

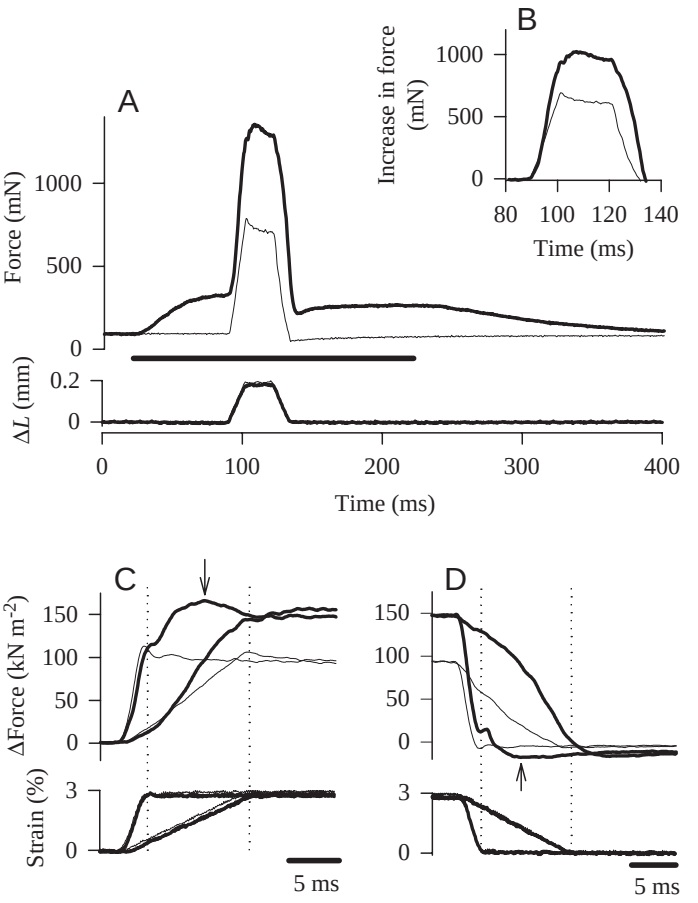

Fig. 6. Force changes in a beetle muscle during ramp stretch and release. Force and length (*L*) traces for the unstimulated muscle are shown as thin lines, those from the tetanically stimulated muscle are the thicker lines. (A) Stretch and release imposed on a muscle when unstimulated and during tetanic stimulation. The total length change was 0.185 mm, and the stretch and release velocity was 15 mm s^{-1}. The time of muscle stimulation (1 ms pulses at 100 Hz) is marked by the horizontal bar beneath the force traces. (B) The increase in force above the pre-stretch level during the stretch and release. (C) Muscle force during stretch, on an expanded time scale, for stretches at 15 mm s^{-1} and at 75 mm s^{-1}. The dotted vertical lines mark the end of the fast and slow stretches. The arrow indicates the time of peak force during the delayed activation following the fast stretch. (D) Decrease in force during shortening at 15 mm s^{-1} and at 75 mm s^{-1}. The dotted vertical lines mark the end of the fast and slow releases. Note that the minimum force reached after the fast release (upward-pointing arrow) comes well after the end of the length change.

deactivation. The force in an unstimulated muscle, as expected for a passive element, fell steadily during shortening and remained more-or-less constant after the end of shortening (Fig. 6D). In a stimulated muscle, the force dropped rapidly during shortening, but then continued to drop to a minimum reached well after the end of shortening. The continued drop in force after shortening reflects delayed deactivation.

Figs 4 and 6 also illustrate another feature that is apparently common to asynchronous muscles, high resting stiffness (see discussion in Josephson et al., 2000). Synchronous muscles,

such as vertebrate skeletal muscles, are relatively compliant when unstimulated and become stiff, resistant to stretch, when stimulated. The beetle muscle is rather different from synchronous muscles in that its stiffness, as judged by the trajectory of the force increase early in stretch, is similar in passive and in active muscle. With the short, fast stretches of Fig. 6C, the force rise is nearly identical in the stimulated and in the unstimulated muscle, indicating similar stiffness in the two. With the slower stretch of Fig. 6C, the force rise is initially similar in the stimulated and unstimulated muscle, but the force trajectories diverge later, with the force rising more rapidly in the stimulated muscle. It seems likely that some, if not all, of the separation of the force trajectories of the unstimulated and stimulated muscle is a result of delayed stretch activation in the latter.

Muscle activation during tethered flight

Muscle action potentials were recorded from a basalar muscle in animals that flew while attached to a force transducer by the dorsal pronotum. The transducer measured the force resulting from wing movements. The basalar muscle has a number of motor units (see above), and the electrical recordings were often rather complex. An experiment was deemed successful if the animal flew and if there was at least one motor unit whose electrical signals were large and repeatedly identifiable in the electrical recording. In the first five successful experiments, the animal was linked to the transducer by way of an insect pin mounted perpendicularly to the transducer blade. The force records in these animals included components of both lift and thrust. In a subsequent set of experiments, five of which were rated as successful, the force recording was improved by mounting the animal directly to the transducer blade such that the force signal represented lift alone (Fig. 7). Values for the frequency of wing strokes and muscle action potentials are based on analysis of five segments, each 0.5–1 s in duration, from each animal.

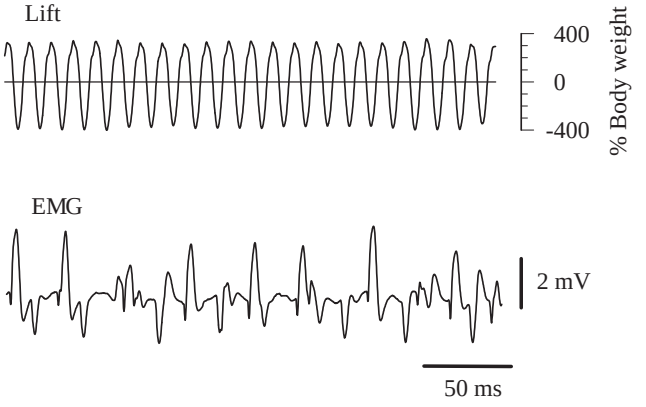

Fig. 7. Lift generated by wing strokes (upper trace) and muscle action potentials recorded from a basalar muscle (EMG; lower trace) during tethered flight. The horizontal line through the lift trace is zero lift, i.e. the force on the transducer when the beetle hung passively from it.

The wing-stroke frequency recorded from animals in tethered flight was 77.6±9.2 Hz (mean ± S.D., *N*=10 animals). Measurements of electromyographic (EMG) frequency were made from the motor unit with the largest electrical signal. The firing frequency of the largest unit averaged 21.1±12.0 Hz (mean ± S.D., *N*=10 animals). While it seems likely that the EMG spikes that we measured were from a single unit in each preparation, it is possible that in some preparations there were two or more motor units producing spikes of similar large size that were counted together, which would make the measured frequency an overestimate of the firing frequency of a single motor unit. As is characteristic of asynchronous muscles, there are many oscillatory muscle contractions for each electrical event.

The lift generated by the wing strokes went through large, nearly sinusoidal oscillations about the zero line. The maximum upward and downward forces were both over three times the animal's body weight (Fig. 7). An average lift of 100 % of body weight would be required to keep the animal airborne in free flight. In tethered animals, the lift averaged over many cycles was only approximately 20 % of body weight (19.8±9.4 %, mean ± S.D., *N*=5 animals). The power output of the tethered animals was substantially less than that required to keep them airborne in free flight.

The determinants of power output

The obvious variables affecting mechanical power output by an asynchronous muscle are muscle length, strain amplitude, strain trajectory (i.e. sinusoidal, sawtooth, symmetrical or asymmetrical, etc.), cycle frequency, muscle temperature and the degree of muscle activation which, in living muscles, is presumably determined by the frequency of activating stimuli (in a synchronous muscle, the degree of muscle activation would be replaced as a variable by the pattern and phase of activation in the strain cycle). The following considers the effects of changes in most of these variables on work and power output. To make the task of evaluating the determinants of work output more manageable, we used sinusoidal strain throughout and have not considered the effects of strain trajectory.

The method for measuring work output

The usual approach used to quantify the effects of changes in a selected variable on mechanical work output is illustrated in Fig. 8. A basalar muscle was stimulated tetanically and subjected to a series of sinusoidal length changes (=strain) imposed during the plateau of the tetanic contraction. The control signals to the ergometer that produced the length changes were generated by a computer. In most experiments, the sinusoidal amplitude, the frequency or the muscle length at mid-cycle was changed by a predetermined amount after every third cycle. Thus, the sinusoidal waveform consisted of a continuous series of three-cycle sets, with a progressive change in the value of one variable between sets. In Fig. 8, it is the strain amplitude that was altered between sets. A single trial, such as that illustrated in Fig. 8A, consisted of 6–8 sets, and thus 18–24 sinusoidal cycles. Varying the value of a variable

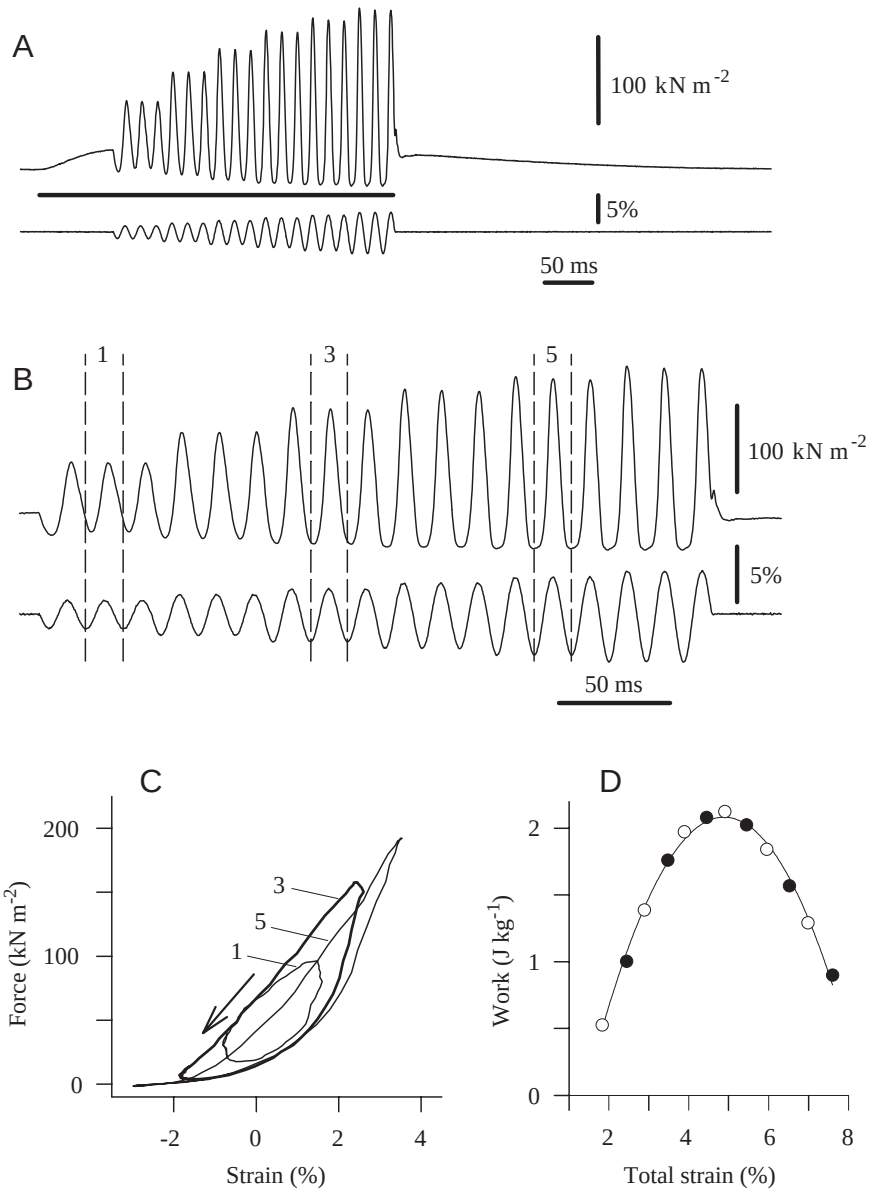

Fig. 8. Measuring the work per cycle and the optimum strain from a beetle muscle. (A) A muscle was stimulated tetanically (stimulus duration marked by the horizontal bar) and, during the contraction, subjected to 60 Hz sinusoidal strain whose amplitude was increased after every third cycle. The upper trace is the muscle force, the lower trace the strain imposed on the muscle. (B) The traces in A on an expanded time base. The middle cycles from the first, third and fifth sets are indicated by vertical broken lines. (C) The work loops formed by the cycles identified in B. The area of each of these work loops is the net work output per unit muscle volume over the cycle. These work loops were traversed in a counterclockwise direction (arrow), indicating positive work output by the muscle. (D) Work per cycle as a function of peak-to-peak strain. The filled symbols are from the traces shown in A and B, and the open symbols are from a similar trial in which the initial strain value was adjusted so that the tested strains from the two trials were interleaved. The continuous line is a second-order polynomial fitted to the data to allow objective determination of the optimal strain (here approximately 5 %) and the maximum work output (approximately 2.1 J kg^{-1} $cycle^{-1}$).

during a trial gave us multiple determinations of the effects of that variable during a single trial. A variable that was changed progressively within a single trial will be referred to as a within-trial variable, as opposed to a between-trial variable, which was altered between trials. Values of muscle length and force during a trial were collected by a computer (sampling rate 15 kHz). A computer program, written in LabVIEW (National Instruments Corp, Austin, TX, USA), generated the sinusoidal control signals, identified the second cycle in each set, displayed this cycle as a work loop (Fig. 8C), and calculated and displayed relevant features of the loop (maximum and minimum muscle length, maximum and minimum force, cycle frequency, work done). The program, designed for measuring work from asynchronous and synchronous muscles, is available from the authors by request. This program requires a PC computer, LabVIEW 5.0 and an appropriate A/D board.

Experimental trials in which there was tetanic stimulation were spaced regularly at 2 min intervals. Several pacing trials, in which the muscle was stimulated tetanically while held at constant length, preceded the series of trials in which data on work performance were collected. Occasionally, trials without stimulation, intended to evaluate the mechanical properties of a passive muscle, were interposed in the interval between trials with stimulation. Muscles were moistened periodically with locust saline throughout an experiment. The thoracic temperature in all experiments was maintained at 35 °C unless stated otherwise.

Each experiment began with a determination of the stimulus intensity needed to activate the muscle fully and, in most experiments, an evaluation of the optimal muscle length and strain for work output. The appropriate stimulus intensity was determined by stimulating the muscle with a brief tetanic burst (1 ms shocks at 100 Hz, 150 ms burst duration). The stimulus

intensity, which was initially subthreshold, was doubled from trial to trial (intertrial interval 1 min) until the evoked isometric contraction reached a maximum. The stimulus intensity used in experiments was twice the minimal intensity needed to produce a maximal response. The procedure used to identify an appropriate muscle length and strain was as follows. The muscle was set initially at a length judged visually to be slightly shorter than the *in vivo* length. The muscle was then stimulated tetanically and, during the plateau of the tetanic contraction, subjected to a burst of sinusoidal strain, usually at 60 Hz. The initial strain amplitude was chosen to be close to the expected optimal value, on the basis of the animal's size. The muscle length was increased after every third cycle of the strain series, typically by 0.02 mm (approximately 0.3 % of muscle length). The muscle length was then set at the length that had given the greatest work in this series. Next, the optimal strain was determined as in Fig. 8. The muscle was stimulated tetanically and subjected to 60 Hz sinusoidal strain, the amplitude of which was increased progressively through the burst. If the strain that gave the greatest work output was found to be significantly different from the initial, estimated value for optimal strain, the optimal length was redetermined using the new value for optimal strain. Trials in which length was varied alternated with those in which strain was varied until optimal values for both variables were established.

The relationship between work output per cycle and either muscle length or the amplitude of imposed strain was an inverted U-shaped function (e.g. Fig. 8D), as was the relationship between power output and cycle frequency. The optimal value of the independent variable (length, strain or frequency) in trials giving results such as that in Fig. 8D was determined by fitting a second-order polynomial to the data using the analysis routine in the plotting program SigmaPlot (SPSS, Inc., Chicago, IL, USA). The second-order polynomial was differentiated, the differential was set equal to zero, and the resulting equation was solved to obtain the optimal value of the independent variable. The optimal value of the relevant variable was substituted back into the original second-order polynomial to obtain the maximum work or power output, that at the optimal value of the independent variable. As a check on this procedure, the maximum power output predicted by curve-fitting in one set of experiments was compared with the maximum power output actually recorded. The experiments used in this comparison were those in which maximum power at the wing-stroke frequency and thoracic temperature of free flight was determined as a function of muscle strain (see below). The mean maximum power predicted by curve-fitting in 12 preparations was 125 W kg^{-1}, the mean of the maximum power actually measured in the 12 preparations was 127 W kg^{-1}. The difference between the maximum measured power and the predicted maximum power was +1.9±3.3 % (mean ± S.D.). Determining maximum work or power by fitting a polynomial to the recorded data does not introduce a significant error. It is not surprising that the measured maximum values are slightly greater than those predicted by curve-fitting. Because of experimental noise, some data points are expected to lie below and some above a fitted curve, and the largest of the measured points is likely to be one of those above the curve.

In many experiments, the principal between-trial variable was presented in either an increasing or a decreasing series, followed by a mirror series in the reverse order. For example, in the next set of experiments to be considered, the between-trial variable was cycle frequency. In half of these experiments, optimal muscle strain (the within-trial variable) was determined in a series of trials at increasing cycle frequency, followed by a second, similar series of trials at decreasing cycle frequency. In the other half of the experiments, the first series was of decreasing frequency and the second of increasing frequency. In these experiments, each series took approximately 30 min to complete. There was some deterioration in the preparations over the course of an experiment and, in all cases, no matter what the between-trial variable, the maximum work per cycle was consistently less in a second series than in the first. In the experiments in which cycle frequency was the between-trial variable, the mean reduction in the maximum work per cycle between the first and second series was 24 % (range 12–38 %). Since the two series were not equivalent, at least for work output, it seemed inappropriate to combine them as we had intended to do when planning the experiments. Therefore, in these experiments, and in similar experiments involving other between-trial variables, the results to be reported are from the first series alone.

Work output as a function of strain and cycle frequency

Optimal muscle strain was evaluated at cycle frequencies of 30, 40, 50, 60, 80 and 100 Hz. The muscle length throughout was that determined to be optimal at 60 Hz. The muscle was

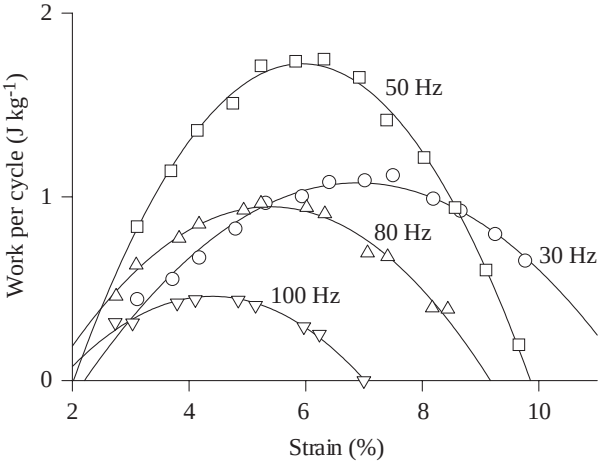

Fig. 9. The relationship between the amplitude of imposed strain and the work done per cycle, measured at different cycle frequencies. The symbols are individual data points, and the continuous lines are second-order polynomials fitted to these points. The optimal strain was obtained by differentiating the second-order polynomial, setting the resulting differential to zero, and solving the equation. Results obtained with cycle frequencies of 40 and 60 Hz in this experiment have been omitted for clarity.

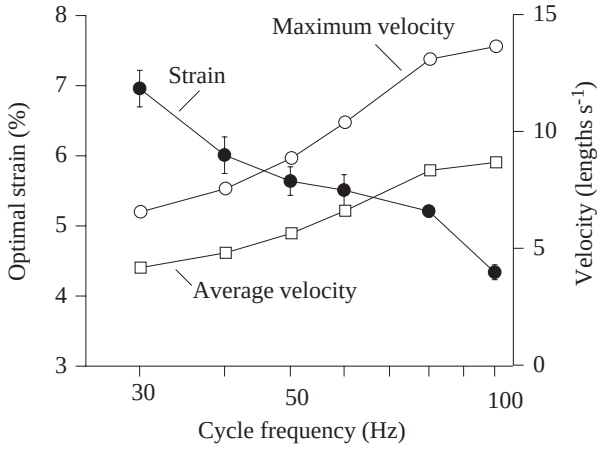

Fig. 10. Optimal strain (filled symbols, means ± 2 S.E.M., *N*=6) and shortening velocities at the optimal strain (open symbols) at different cycle frequencies. Maximum velocity (=π*FS*, where *F* is cycle frequency and *S* is peak-to-peak strain) is indicated by circles, and mean velocity during shortening (=2*FS*) is indicated by squares.

subjected to two sets of strains with interleaved values at each frequency (see Fig. 8D). Six animals were used in these experiments. In three preparations, the first frequency used was 30 Hz, and the frequencies were progressively increased through the series; in the other three preparations, the frequencies were presented in descending order.

The work output per cycle was strongly dependent on strain, and there was an obvious optimal strain at each cycle frequency examined (Fig. 9). The optimal strain declined progressively as the cycle frequency increased, falling from approximately 7 % at 30 Hz to 4 % at 100 Hz (Fig. 10). The width of work *versus* strain curves also declined progressively with increasing cycle frequency (Fig. 11). The work per cycle at the optimal strain was greatest at the 50 Hz cycle frequency

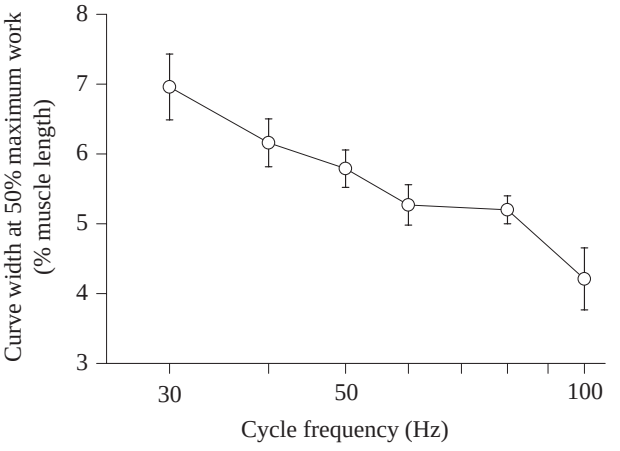

Fig. 11. The width of work *versus* strain curves, such as those of Fig. 9, at different cycle frequencies. The width of each curve was measured at 50 % of the maximum work for that curve. Values are means ± 2 S.E.M., *N*=6.

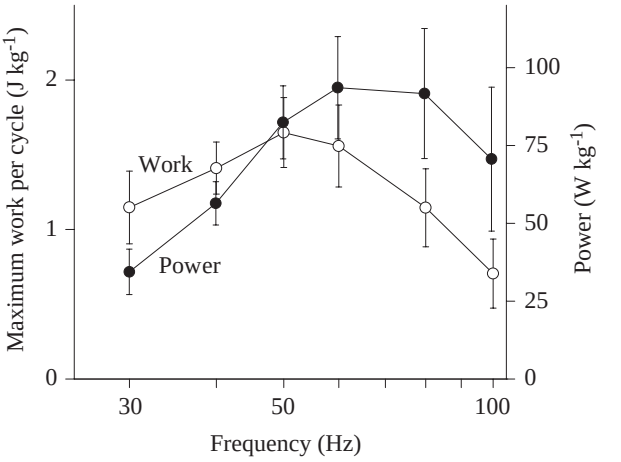

Fig. 12. Maximum values of work per cycle and net power output during sinusoidal length change at different frequencies. Values are means ± 2 S.E.M., *N*=6.

(Fig. 12). Mechanical power output, which is the product of work per cycle and cycle frequency, rose with increasing cycle frequency to reach a maximum at 60–80 Hz, and declined when the frequency was increased further to 100 Hz (Fig. 12).

The usual inverse relationship between muscle force and shortening velocity dictates that there is an optimal shortening velocity for mechanical power output. If a muscle is to operate at or near this optimal velocity while shortening, there should be an inverse relationship between the cycle frequency and the strain per cycle. There is a decrease in optimal strain with increasing cycle frequency in the beetle muscle, but the decline in optimal strain with increasing cycle frequency is not great enough to result in the muscle operating at a single, optimal shortening velocity across the frequency range examined. The maximal velocity reached during a sinusoidal length trajectory and the mean velocity during the shortening portion of the cycle are both proportional to the product of strain and cycle frequency, and both measures of velocity increase with increasing cycle frequency for muscle operating at the optimal strain (Fig. 10).

Work output as function of muscle length

In this group of experiments, the within-trial variable was muscle length. The length was initially set well below that anticipated to be optimal for work output, and the length was increased from set to set throughout the trial in steps that were great enough that the length passed through and beyond the optimum. The relationship between muscle length and work output was determined at a series of strains, ranging from approximately 2 to 10 %, and at cycle frequencies of 40, 60 and 90 Hz. This experiment was repeated with four preparations, each of which gave basically similar results leading to the following conclusions.

(i) At normal operating frequencies, the work output is positive over only a very limited range of muscle length (Fig. 13). In the experiment shown in Fig. 13, the maximum work per cycle occurred at the 60 Hz cycle frequency and with

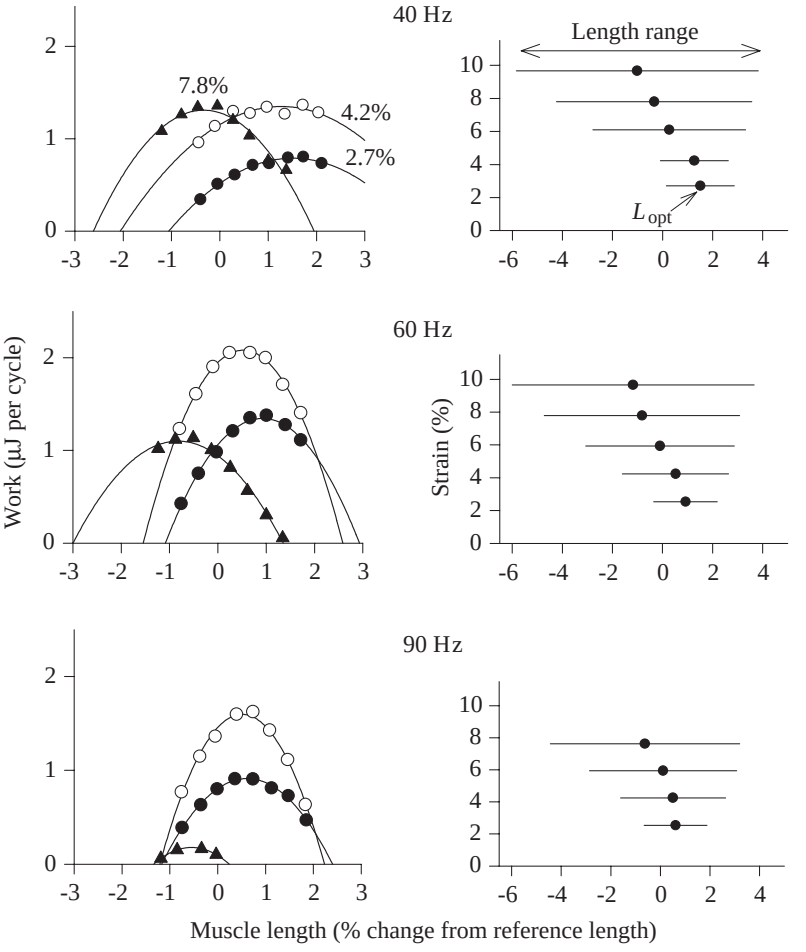

Fig. 13. The relationship between muscle length and the work done per cycle, measured at different muscle strain and cycle frequency. The reference length used in the abscissa of all panels was that length found to be optimal for work output at 60 Hz in the set-up trials before the main experiment. Left-hand panels: work output as a function of muscle length at three different strains. These results are from an experiment in which muscle length was changed progressively during a trial. In each panel, the results from a single trial are shown by a common symbol. The continuous lines are second-order least-squares regressions fitted to the results of a trial. The numbers above the data sets in the upper left-hand panel show the peak-to-peak strain for that data set and for the data sets with the same symbol in the two panels below. Some sets of data were obtained at different strain levels from those shown but, to increase the clarity of the presentation, they have not been plotted. The three panels show results obtained at cycle frequencies of 40, 60 and 90 Hz as indicated. Right-hand panels: optimum muscle length for work output (L_{opt}, filled symbols) and the length changes experienced by a muscle during sinusoidal strain cycles when operating at the optimum length for different strains and cycle frequencies (horizontal lines). The optimal muscle lengths were obtained by differentiating the second-order polynomials shown as continuous curves in the left-hand panels, setting the resulting differentials to zero, and solving the equations.

muscle strain of 4.2 %. The curve of work output *versus* muscle length for these values of frequency and strain in Fig. 13 (left-hand column, middle panel, open circles) has a width measured at half-maximal work of only 2.9 %. In the three other experiments of this series, the width, measured similarly, of that work *versus* length curve with the greatest maximum work at 60 Hz was 2.7 or 2.8 %.

(ii) The work *versus* muscle length curves become increasingly narrow as cycle frequency is increased (Fig. 13). The mean width of the curves with the greatest peak work, again measured at half-maximal work, was 4.9 % (range 3.9–6.5 %) at 40 Hz, 2.8 % (range 2.7–2.9 %) at 60 Hz and 2.7 % (range 2.4–2.9 %) at 90 Hz.

(iii) The optimal length for work output declines as strain is increased (Figs 13, 14). The change in optimal muscle length with increasing strain is such that, if the muscle is at optimal length at mid-cycle, the maximal length reached during stretch increases little with increasing strain, while the minimal length reached during shortening declines substantially.

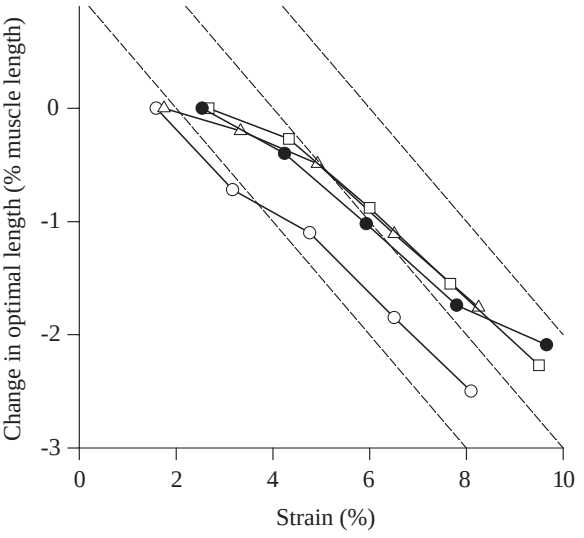

Fig. 14. Change in optimal muscle length with increasing strain, relative to that at the smallest strain tested; cycle frequency 60 Hz, temperature 35 °C. Each set of symbols joined by a line is from a single preparation. Data shown by the filled symbols are from the same preparation as in Fig. 13. The diagonal broken lines have a slope of −1/2 and are given for reference. The maximum muscle length reached in a cycle is the initial length plus half the peak-to-peak strain. For the maximum muscle length reached in a cycle to remain constant, the initial muscle length should decrease with increasing strain by an amount equal to half the strain; i.e. with the slope shown by the broken lines.

Optimal cycle frequency and power output at different temperatures

In these experiments, cycle frequency was the within-trial variable and temperature was the between-trial variable. To increase resolution, pairs of trials, the second of which had values that interdigitated with the first, were given at each temperature. The muscle length and strain amplitude were those found to be optimal for work output in a series of test trials at 30 °C and a cycle frequency of 50 Hz. The test trials immediately preceded the experimental trials in which cycle frequency and temperature were varied. The temperatures used were 25, 30, 35 and 40 °C. In three preparations, the temperatures were presented in increasing order, in three preparations in decreasing order.

The optimal cycle frequency and the power output at that frequency increased in parallel with increasing muscle temperature (Figs 15, 16). The limits of the frequency range over which there was positive power output were not explored, but it was clear that the curves relating cycle frequency and power output were rather broad, with positive power over at least a fourfold range of frequencies. The peak power output in these experiments, that at 40 °C and 60–70 Hz cycle frequency, was slightly greater than 100 W kg^{-1} (104±24 W kg^{-1}, mean ± S.D.).

Optimal strain, work per cycle and power output at different temperatures

The following experiments were performed to characterize better the effects of temperature on work output by the muscle. The within-trial variable was strain; the between-trial variables were cycle frequency (40, 60 and 90 Hz) and temperature (25–40 °C in steps of 5 °C). In three preparations, the three cycle frequencies were presented during each of a set of increasing temperatures; in three preparations, the temperatures series was decreasing.

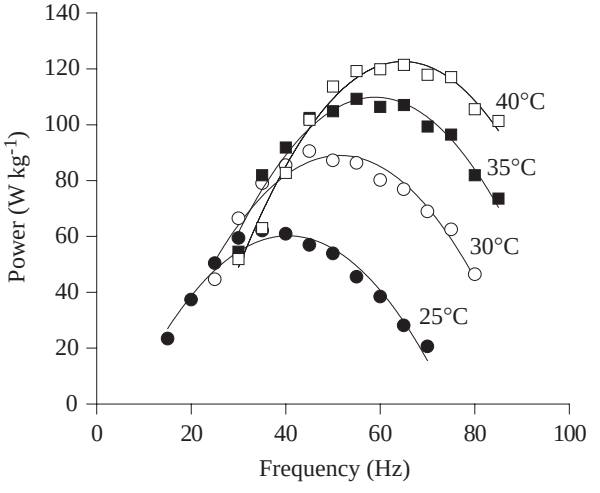

Fig. 15. The effects of changing cycle frequency on mechanical power output measured at different temperatures. The muscle length and strain were those determined to be optimal for work output at 30 °C and a cycle frequency of 60 Hz. The temperatures in this example were presented in decreasing order.

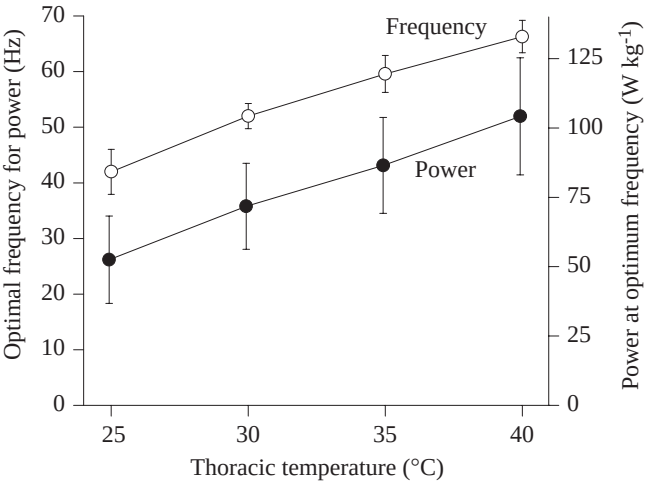

Fig. 16. Effects of temperature on the optimal frequency for power output and the power output at the optimal frequency. The results are from experiments such as that in Fig. 15. Values are means ± 2 S.E.M., N=6. The Q_{10} values for the temperature range 25–40 °C were 1.4 for optimal frequency and 1.6 for power output.

At least in synchronous muscles, shortening velocity is strongly dependent on temperature, with Q_{10} values for maximum shortening velocity typically being 1.5–3 in the normal range of operating temperatures (Bennett, 1984). Therefore, we anticipated that the optimal strain at a given cycle frequency would be strongly dependent on muscle temperature and that the work per cycle would increase with temperature. We reasoned that, because of a higher shortening velocity, the optimal distance of shortening during a cycle, and therefore the optimal strain, would increase with increasing temperature and that the greater strain would lead to greater work output. In fact, the optimal strain was found to be only weakly dependent on temperature (Fig. 17A). Increasing the temperature from 25 to 40 °C increased the optimal strain by only 24 %, 23 % and 40 % at cycle frequencies of 40, 60 and 90 Hz respectively. Further, although the work per cycle did increase monotonically with increasing temperature at the 90 Hz cycle frequency, at 40 and 60 Hz, the work per cycle at optimum strain passed through a maximum and then declined with further increase in temperature (Fig. 17B). There was a general tendency for the maximum power output at 40, 60 or 90 Hz to increase with temperature, but the peak power at 40 °C (94 W kg^{-1} with 90 Hz cycle frequency) was not significantly greater than that at 35 °C (93 W kg^{-1} with 60 Hz). The relative insensitivity of optimal strain to temperature change and the complex relationship between work output and temperature probably result from temperature affecting, sometimes in contradictory ways, both muscle shortening velocity and the time course of the deactivation processes that underlie asynchronous operation. We will return to this in the Discussion.

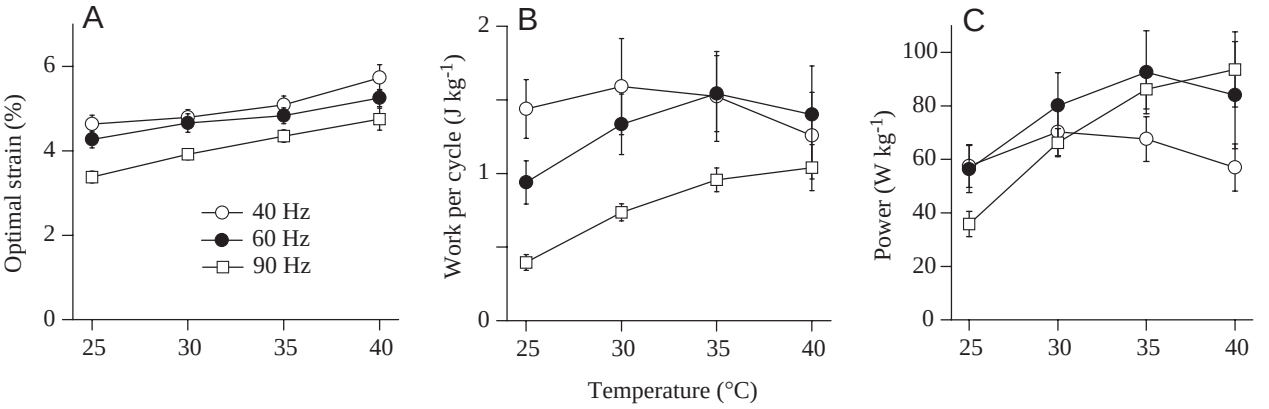

Fig. 17. The effects of temperature on optimal strain (A), on the work per cycle (B) and on power output (C) at the optimal strain. To reduce overlap in the error bars, the results are shown as means ± 1 S.E.M., rather than as means ± 2 S.E.M. as in preceding figures (N=6). The Q_{10} values for optimal strain over the temperature range 25–40 °C were 1.15, 1.15 and 1.25 for strain frequencies of 40, 60 and 90 Hz respectively.

Force and power as functions of stimulation frequency

These experiments were performed as part of the study in which maximum power output was determined at the wingbeat frequency and thoracic temperature of free flight (see below). The strains and muscle lengths used were those found to be optimal at the thoracic temperature and wing-stroke frequencies determined during flight for each of the individual animals. The maximum isometric force and the power output during cyclic strain at 90 Hz were determined as the muscle was stimulated at 20, 50, 100 and 200 Hz. Isometric force was that measured in a tetanic contraction initiated 2 min before the work trial. Muscle temperature was 35 °C. In three preparations, the stimulation frequencies were presented in ascending order, in another three in descending order. The cycle frequency of 90 Hz was chosen because it is close to the wing-stroke frequency measured from freely flying insects (mean 94 Hz; see below). It was thought that evaluating the effects of the frequency of muscle activation on power output would be most relevant to muscle performance during flight if the cycle frequency used was similar to that during flight.

At stimulus frequencies of 100 and 200 Hz, the individual responses to stimuli were completely fused, and the isometric force during stimulation reached a smooth plateau. However, with stimulus frequencies of 20 Hz, and to a lesser extent with 50 Hz, there was incomplete force fusion, and the isometric force trace had ripples at the stimulation frequency. At 20 Hz, the amplitude of the force ripples was 25.6±6.6 % of the peak force (mean ± S.D.); at 50 Hz, the ripples averaged 6.3±1.8 % (mean ± S.D.) of the peak force.

The maximum isometric force and the mechanical power output both increased with increasing stimulus frequency in the range 20–100 Hz (Fig. 18). The relative increase in power output over this range of stimulus frequencies (mean factorial increase 3.8±1.2, mean ± S.E.M., N=6) was greater than that of force (1.9±0.3, mean ± S.E.M.), but the difference in the relative increase in power and force was not statistically significant (P>0.14, two-tailed t-test). Increasing the stimulus frequency from 100 to 200 Hz resulted in a slight, but not statistically significant, decrease in power output (change in power −2.1±8 %, mean ± S.E.M.) and a small, but statistically significant, increase in isometric force (force increase 6.1±2.4 %, mean ± S.E.M.; P<0.05).

Estimating power output during flight

In this series of experiments, the maximal power output from the basalar muscles of a series of animals was measured at the wingbeat frequencies and the thoracic temperatures of the same animals during free flight. The flight frequency was determined with an optical tachometer or by recording the flight tone with a microphone. Unambiguous recordings of wing-stroke frequency were obtainable with either the tachometer or the microphone (Fig. 19), but we found measurements to be made more easily with the microphone, and this was used in most experiments.

An animal from which recordings of wing-stroke frequency

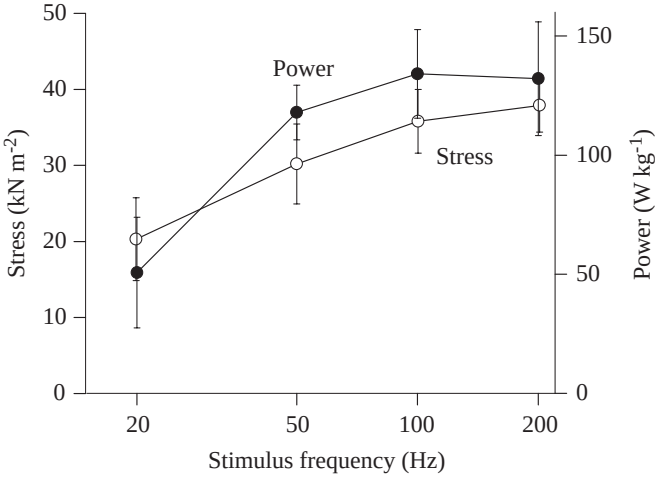

Fig. 18. Isometric stress (increase above unstimulated level) and power output (cycle frequency 90 Hz) as functions of the stimulation frequency used to activate the beetle muscle at 35 °C. Values are means ± 2 S.E.M., N=6.

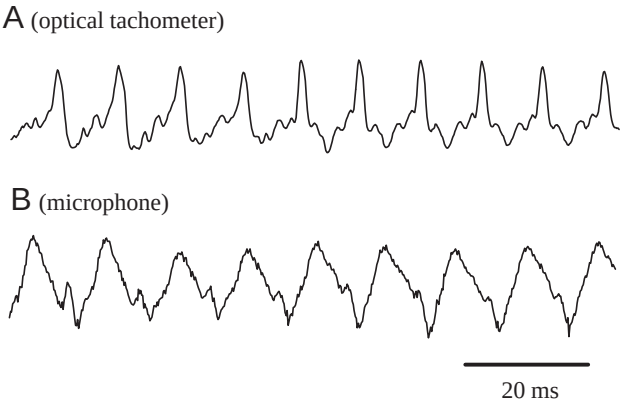

Fig. 19. Wing strokes recorded with an optical tachometer (A) or, from another animal, as flight tone (B).

and thoracic temperature had been obtained was prepared for muscle work measurements in the usual way. An appropriate stimulus intensity was determined with the animal at 30 °C, and the preparation was then warmed to the thoracic temperature measured for flight. Using, as a cycle frequency, the mean wing-stroke frequency of flight, trials in which muscle length was the within-trial variable were alternated with trials in which strain was the within-trial variable until optimal values of muscle length and strain had been identified. The results from this experiment are summarized in Table 2. The mean wingbeat frequency during flight was 94 Hz, and the mean thoracic temperature was 35 °C. The mean power output at the wing-stroke frequency and thoracic temperature of free flight was 127 W kg^{-1} (Table 2). Two of the preparations in Table 2 had maximum power values (57 and 40 W kg^{-1}) that were distinctly smaller than the others, probably because of some untoward effect of the experimental manipulations made during measurements. When these two preparations are excluded, the mean power output was 141 W kg^{-1}.

Table 2. *Wing-stroke frequency and thoracic temperature during free flight, and maximal muscle power output measured at that frequency and temperature*

	Body mass (g)	Wingbeat frequency (Hz)	Thoracic temperature (°C)	Maximum power (W kg^{-1})
	1.4	87	35.2	199.8
	1.5	93	36.8	168.3
	1.4	94	34.3	165.7
	1.4	97	35.3	143.9
	1.4	93	34.3	140.1
	1.4	94	35.2	135.6
	1.5	88	34.0	126.5
	1.8	95	35.2	125.3
	1.2	98	34.0	110.3
	1.4	100	30.4	107.1
	1.3	97	36.4	57.1
	1.5	91	37.9	40.4
Mean ± S.D.	1.4±0.1	94.0±3.8	34.9±1.9	126.9±44.9

Values from individual experiments are arranged in order of decreasing maximum power.

Discussion

The power available from asynchronous muscle

The maximum power output of the beetle basalar muscle, measured under conditions simulating those of normal flight, averaged 127 W kg^{-1}, or 141 W kg^{-1} if two suspiciously low values are excluded (Table 2). If all the asynchronous flight muscle of a *C. mutabilis* produced 141 W kg^{-1}, the total power output would be approximately 27 W kg^{-1} animal. The power output from the beetle muscle, an asynchronous muscle, is substantially greater than that measured using the work-loop approach from synchronous flight muscles of insects (68–90 W kg^{-1}; for references, see Introduction), supporting the hypothesis that asynchronous muscle has evolved in a number of insect lines in part because it allows greater mass-specific power output at the high operating frequencies of insect flight.

The increase in power output from the beetle muscle above that available from synchronous flight muscles of insects is greater than can be accounted for by simply replacing the sarcoplasmic reticulum of the synchronous muscles with myofibrils. In locust flight muscle, sarcoplasmic reticulum and T-tubules occupy approximately 10 % of the fiber volume and myofibrils occupy approximately 65 % (Josephson et al., 2000). Thus, replacing sarcoplasmic reticulum with myofibrils in the locust muscle might increase the power output by approximately one-sixth (assuming that some way, other than Ca^{2+} release from the sarcoplasmic reticulum, could be found for turning the muscle on and off), whereas the measured power output from the beetle muscle is approximately twice that of locust flight muscles. Apparently, the mass-specific power output of the myofibrils themselves is greater in the asynchronous muscle of the beetle than in synchronous flight muscles.

The power output from the beetle muscle was also much greater than that recorded earlier from an asynchronous flight muscle of a bumblebee (mean 45 W kg^{-1} at 40 °C, maximum approximately 100 W kg^{-1}; Josephson, 1997b). It seems likely that the difference in measured power output between beetle and bumblebee muscles is a result of different experimental approaches used in the two studies, rather than of differing intrinsic capacity for power output in muscles of the two species. The presence of a distal apodeme on the beetle muscle allowed measuring devices to be attached to the muscle in a manner that better mimicked the normal loading of the fibers within the muscle than was readily achievable with the bumblebee muscle. It is probable that resting lengths of fibers in the beetle preparations and the changes in the lengths of the fibers during imposed strain more closely approximated those in intact animals than was true in the studies of bumblebee muscle, with correspondingly greater power output.

The only muscle preparation of which we are aware in which the directly measured, sustainable power output is as great as

or greater than that of the beetle basalar muscle is the fast glycolytic (FG) portion of the iliofibularis muscle of the lizard *Dipsosaurus dorsalis*. Fiber bundles from the lizard iliofibularis produced 154 W kg^{-1} at an operating temperature of 42 °C and an optimal cycle frequency of 20 Hz (Swoap et al., 1993). A significant part of the space inside muscle fibers is occupied by mitochondria, sarcoplasmic reticulum and glycogen, none of which contributes directly to mechanical power output. An appropriate measure of the work capacity of the contractile machinery itself is the power output per unit mass of myofibril. Myofibrils make up approximately 82 % of the volume of FG fibers of the frog sartorius muscle and the guinea pig vastus muscle (Mobley and Eisenberg, 1975; Eisenberg and Kuda, 1975), and it seems reasonable to assume that the myofibrillar volume is similar in FG fibers of the lizard iliofibularis. Ignoring, for lack of information about it, that fraction of an iliofibularis muscle that is extracellular space gives 188 W kg^{-1} as the mass-specific power output of myofibrils in the lizard muscle. The beetle basalar muscle is an aerobic muscle with abundant mitochondria and, in the beetle muscle, myofibrils make up only approximately 58 % of the fiber volume (Josephson et al., 2000). Using 141 W kg^{-1} as the power output of whole muscle, and again ignoring extracellular space, gives a mass-specific power output for beetle myofibrils of 243 W kg^{-1}, which is, to the best of our knowledge, the highest sustainable power output for myofibrils yet reported.

There are several reasons for believing that the power output of the basalar muscle measured in this study is an underestimate of the maximum power available from the muscle in an intact animal. First, the muscle preparations deteriorated slowly during the course of experiments. In a number of experiments, the muscle was subjected to a paired series of changes in the variable being investigated: changes in an independent variable were presented in an ascending series followed by a mirror series with descending values, or the converse, a descending set was followed by an ascending one. Work or power output at equivalent values of variables was typically 10–40 % less in the second series than in the first. The decline in performance appeared to be gradual. It seems likely that deterioration of the muscle begins early during preparation for mechanical recordings, and that there has been some decline in performance before we make our first measurements. Second, for convenience, and to allow better comparison with results from other work-loop studies, we have used sinusoidal strain in our determinations of work output. A sinusoidal length change may not be the optimal trajectory for mechanical power output from the muscle. Gilmour and Ellington (1993b) found that including a second harmonic in the strain trajectory increased the work output from some glycerinated fibers of bumblebees. In theory, and in fact, a muscle produces approximately 10 % more work per cycle if the length trajectory is a symmetrical saw-tooth rather than a sinusoidal oscillation (Josephson, 1989; Askew and Marsh, 1997). Work output is also expected to increase if the cycle is asymmetrical, with the shortening phase being longer than lengthening (Askew and Marsh, 1997; Girgenrath and Marsh, 1999), but this option is probably not useful for the flight muscles of beetles. Increasing the fraction of a cycle spent in shortening by the basalar, a wing depressor, would necessarily reduce the shortening duration and work output by wing elevators, and there would probably be little or no effect on power output by the flight system as a whole. Third, modulatory substances in the solution bathing a muscle can increase power output from the muscle (Malamud et al., 1988). We used a simple saline, albeit sparingly, to keep the muscle moist, and the saline may have lacked modulatory factors needed for maximal muscle performance. Muscle deterioration, an inappropriate strain trajectory and failure to provide appropriate modulatory factors are all likely to reduce power output below maximal values, but by how much is uncertain. We guess that the mechanical power available from beetle muscle *in vivo* is greater than 150 W kg^{-1}, but probably not more than approximately 200 W kg^{-1}.

Neural control of power output

Motor neuron impulses to an asynchronous muscle lead to muscle fiber depolarization, the release of Ca^{2+} into the fiber cytoplasm, and the creation of a permissive environment in which the myofibrils can contract in an oscillatory manner if linked to an appropriate mechanical load. An asynchronous muscle is not simply turned on or off by neural input or the lack thereof. The frequency of motor neuron impulses to a motor unit of a muscle controls the power output available from the motor unit. Previous studies have provided indirect evidence linking the frequency of activation with the power output of asynchronous muscle. In one of their seminal studies on the physiology of asynchronous muscle, Machin and Pringle (1959) found that the amplitude of the oscillation of a beetle basalar muscle contracting against an inertial load, but not the frequency of these oscillations, increased with an increase in the frequency of muscle stimulation, up to a plateau reached at a stimulus frequency of 20–30 Hz (at 25–30 °C) in different species. Nachtigall and Wilson (1967) demonstrated that the lift generated by flies during tethered flight was correlated with the firing frequency of units in the asynchronous power muscles of the wings. And in honeybees, the rate of oxygen consumption during warm-up and flight is proportional to the action potential frequency in the wing muscles, indicating that the metabolic power output of the muscles, at least, is a function of the neural activation frequency (Bastian and Esch, 1970).

Measurements of power output from the basalar muscle of *C. mutabilis* as the muscle was activated with stimuli at different frequencies demonstrated directly and quite clearly that the power output was dependent on the stimulation frequency (Fig. 18). The mean power output from the six preparations increased by a factor of 2.6, from 51 W kg^{-1} to 134 W kg^{-1}, when the muscle stimulation frequency was increased from 20 Hz to 100 Hz. In addition to varying power by varying the degree of activation of individual motor units, a beetle could, in theory, adjust its power output by recruiting different numbers of motor units to meet varying needs. At

least five excitatory axons and at least one inhibitor innervate the beetle basalar muscle. The function of the inhibitor is unknown, but stimulating it does reduce the isometric tension generated by excitatory axons, and one presumes that power output would be similarly reduced. Potentially, the beetle basalar muscle has a wide dynamic range of power output achieved by varying both the number of participating motor units and the level of excitation of the participating units.

An indication that beetles not only could but actually do control power output by varying the frequency of activating motor neuron impulses was seen in the performance of animals in tethered flight. The frequency of motor unit action potentials in tethered animals was approximately 20 Hz which, judging by the relationship between motor unit activation and power shown in Fig. 18, would have allowed a power output of only approximately 38 % of maximum. Related to, and probably a consequence of, the low activation frequency, the lift produced by the tethered animals was low, approximately 20 % of that needed to counteract the body weight. Low lift production by tethered animals is not unusual (see, for example, Gewecke, 1975; Bauer and Gewecke, 1985) and is probably a consequence of the absence, in tethered animals, of the appropriate visual and tactile cues needed for the control of aerodynamic performance, control exerted in part through adjustment of the impulse frequency to the participating muscles.

Are there several varieties of asynchronous muscle?

On the basis of the information available to him at the time, Boettiger (1960), in his review of the physiology of insect flight muscles, concluded that there were at least two kinds of asynchronous muscle. These were termed Type 1 fibrillar muscle, the prototype of which is the dorsal longitudinal flight muscle of the bumblebee, and Type 2 fibrillar muscle, exemplified by the beetle basalar muscle. The existing evidence suggested that the bumblebee muscle became fully activated when held isometrically and stimulated tetanically, and that stretch did not further increase activation. It was thought that release of an isometrically contracting bumblebee muscle resulted in delayed shortening deactivation and that the recovery from deactivation could be hastened by restretching the muscle to its pre-shortening length. The beetle muscle, in contrast, was thought to become only partially activated when stimulated at constant length. It was proposed that stretch of an isometrically contracting beetle muscle resulted in a delayed increase in the level of muscle activation and that release of the muscle resulted in delayed shortening deactivation. Because of their different responses to stretch and release, the work loops of Type 1 and Type 2 fibrillar muscles were thought to be positioned differently with respect to the passive and stimulated length/tension curves for the muscles. The work loops of the Type 1 muscles were said to lie between the passive and active length/tension curves, while the work loops for the Type 2 muscles were thought to overlap the stimulated length/tension curve, but with the major axis of the loop rotated clockwise with respect to the length/tension curve such that the force at the longest length reached in the loop lay below, and that at the shortest length lay above, that expected from the force during an isometric tetanic contraction.

We have now examined asynchronous muscles from both beetles and bumblebees using basically the same techniques (bumblebee results are presented in Josephson and Ellington, 1997; Josephson, 1997a,b). We conclude that asynchronous muscles from beetles and bumblebees are remarkably similar. The responses of both muscles to imposed stretch and release are quite similar (compare Fig. 1 in Josephson, 1997a, with Fig. 6 in the present study). In bumblebee flight muscles as well as in beetle basalar muscles, there is both delayed, transient stretch activation and delayed, transient shortening deactivation. Both beetle and bumblebee muscles show pronounced stress relaxation (Fig. 5), which makes determinations of length/tension curves for stimulated and unstimulated muscle rather problematical. The positions of length/tension curves, as we determined them, and work loops were essentially the same in bumblebee and beetle muscles. In both beetles and bumblebees, work loops from stimulated muscles overlapped the stimulated isometric length/tension curve, and the work loops were rotated counterclockwise with respect to the curve (see Fig. 8 in Josephson, 1997a; Fig. 4 in the present study). It may well be that substantially different mechanisms underlie asynchronous oscillation in some of the many independent inventions of this mode of operation in different insect groups, but our results from bumblebees and beetles do not support the suggestion of Boettiger (1960) that there are fundamentally different types of asynchronous muscle.

Muscle length, strain and cycle frequency

If a basalar muscle is maintained at constant temperature, stimulated at an intensity and frequency adequate to activate it fully and subjected to sinusoidal strain, the work output by the muscle is determined by the values of three interacting variables: the amplitude of the strain, the background muscle length upon which the strain is superimposed and the frequency of the strain cycle. There is an interesting, inverse relationship between strain amplitude and the optimal muscle length for work output. As strain is increased, the optimal muscle length decreases by just about the amount required to keep constant the maximum muscle length reached at the peak of the strain (Figs 13, 14). The range of strain amplitude, and of muscle length, over which there can be substantial work output is quite narrow. At a cycle frequency of 80 Hz, which is close to the normal wing-stroke frequency during flight (mean 94 Hz), the width of the curve relating work output and strain, measured at half-maximal work output, occurs at a strain that is only approximately 5 % of the resting muscle length (Figs 9, 11). The width at the half-maximum of the curve relating work and muscle length, measured at 90 Hz and with optimal strain, is slightly less than 3 % of resting muscle length (Fig. 13). The relationship between work output and muscle length is much narrower, and the peak occurs at a shorter muscle length, than the force/length curve for either

isometric twitch or tetanic tension (Fig. 4). The capacity for work output is well below maximum at the optimal muscle length for force production; why this is so is unknown. The work *versus* muscle length and work *versus* strain curves for asynchronous flight muscle of the bumblebee are also quite narrow. In bumblebee flight muscle, the width at half-maximum of the work *versus* strain curve is approximately 2.5 % of muscle length, and that for the work *versus* length curve is 3.9 % of muscle length (Josephson, 1997a). On the basis of this admittedly limited sample, it appears that positive power output in asynchronous muscle is available over only a very limited operating range of muscle length and strain.

Muscle power output rose with operating frequency to a broad maximum reached at 60–80 Hz and then fell with further increase in frequency (Fig. 12). The wingbeat frequency that the beetle uses while flying, approximately 94 Hz, appears to be slightly higher than the frequency range over which the muscle power output is maximal. The optimal strain for power output declined monotonically over the range of cycle frequencies examined. The optimal muscle strain measured at the normal wingbeat frequency of flight is 4–5 % of resting muscle length (Figs 11, 17).

Can fiber strain be uniform throughout the muscle?

The fibers of the basalar muscle insert dorsally on a cuticular cap and ventrally on the sternum. The sternum is curved, which results in variation in fiber length across the muscle. The most lateral fibers are slightly more than 4 mm long, the most medial slightly more than 7 mm (Fig. 1). The work output from the muscle as a whole, and one expects from each of the fibers individually, during cyclic shortening and lengthening is strongly dependent on the fractional length change (=strain) experienced by the muscle and its fibers. Although there is variation in fiber length throughout the muscle, it is possible, and we think likely, that fibers throughout the muscle operate at similar strain during the cyclic shortening and lengthening of the muscle during flight.

A short apodeme, originating roughly in the center of the cap to which the muscle attaches dorsally, connects the muscle to the wing base. The cuticular cap is relatively free to pivot at the junction with the apodeme, and it may be expected to do so if the force distribution on the cap is unbalanced with respect to the attachment point of the apodeme. The fibers of the muscle are stiff, both when passive and when stimulated. Because of their high stiffness, differences in strain between fibers in different parts of the muscle would result in large differences in force, which would in turn lead to pivoting of the cuticular cap on the apodeme in a direction that tended to balance the force in different sectors of the muscle insertion. The cuticular cap would not have to pivot very much to maintain strain equality among the different fibers of the muscle during imposed length changes. If all the fibers of the muscle were uniformly strained by 5 %, the lengths of the longest fibers of the muscle would increase from 7 to 7.35 mm and those of the shortest fibers from 4 to 4.2 mm. The muscle has a cross-sectional area of approximately 6.6 mm^2. If it is assumed that the muscle is circular in cross section with a diameter of 2.9 mm, and that the longest and shortest muscle fibers attach at opposite sides of the circular cap, the cap would end up, after the imposed strain, slanted by only 3 ° from its resting position. The insertion of the muscle upon a cap that can pivot potentially allows the muscle fibers, even though of differing lengths, to operate at similar strain.

Temperature and muscle performance

Isometric contractions of the beetle basalar muscle were not much changed by increasing muscle temperature from 30 to 40 °C. Twitch tension declined insignificantly, tetanic tension increased slightly, and twitch rise and decay times were somewhat shortened (Table 1). The effect of an increase in temperature on the twitch tension developed by a muscle is dependent on the balance between two opposing factors: a decline in the duration of muscle activation with increasing temperature, and an increase in the rate of tension development while the muscle is active. The net effect of temperature change on the twitch tension in different muscles is variable and unpredictable, and it is certainly not uncommon for twitch tension to decline, as it does in the beetle muscle, with increasing temperature (for a review, see Bennett, 1984). Tetanic tension is often not very temperature-dependent, especially at higher temperatures, and the Q_{10} of 1.1 for tetanic tension in the beetle muscle is similar to that of many other muscles (Bennett, 1984). The beetle muscle is unusual, however, in the low thermal dependence of its twitch rise and decay times. The Q_{10} values for twitch rise time (1.2) and decay time (1.7) are substantially smaller than those reported for most other muscles (Bennett, 1984).

Two experimental approaches were used to examine the effects of temperature on power output. In the first, which provided the data for Figs 15 and 16, muscle length and strain were held constant, the within-trial variable was cycle frequency and the between-trial variable was muscle temperature. The results from these experiments were quite straightforward: both optimal operating frequency and maximum power output increased monotonically and approximately linearly with muscle temperature. In the second experimental approach, that of Fig. 17, the within-trial variable was strain and the between-trial variables were cycle frequency and temperature. Here, the effects of temperature were less straightforward. At the lower two of the three frequencies tested (40 and 60 Hz), the work and power output at the optimal strain for each frequency and temperature did not increase monotonically with temperature, but rather rose to a maximum and then declined with increasing temperature. At the highest frequency (90 Hz), the work and power rose continuously with temperature but at a steadily decreasing rate, and it seems likely that the work and power curves at 90 Hz would also have shown an optimal temperature had a larger temperature range been examined.

To account for the temperature optima for work output at low operating frequencies seen in Fig. 17, we propose that the effect of temperature on work output, like the effect of

temperature on twitch force, is dependent on the balance between two opposing factors. For work output, the competing factors are (i) an increase in shortening velocity with increasing temperature and, hence, an increase in the rate of work output during shortening; this is opposed by (ii) a decrease, with increasing temperature, in the durations of the stretch activation and the shortening deactivation that underlie positive work production. We assume that the shortening velocity of the beetle basalar muscle is a positive function of temperature; indeed, it would be surprising if it were not. We have not made any direct measurements of the effects of temperature on the time course of stretch activation and shortening deactivation. Abbott and Steiger (1977) report that the rate constant for the delayed tension change following stretch and release in glycerinated fibers of *Lethocerus* flight muscle has a high Q_{10}. Interestingly, in the *Lethocerus* fibers, the stretch activation and shortening deactivation were maintained and did not decay rapidly with time as they clearly do in the beetle basalar muscle (Fig. 6). Perhaps the apparent difference between bug and beetle muscle is a consequence of the quite different strains used in the two studies (<0.4 % with *Lethocerus*; 3 % and more with ramp stretch and release of the beetle muscle). We assume that the rise and decay times of the delayed activation processes in the beetle muscle are temperature-dependent and that increasing temperature leads to a shorter total duration of stretch activation and shortening deactivation; again, it would be surprising if this were not the case.

Consider experiments such as those whose results are shown in Fig. 17. We hypothesize that, at temperatures below the optimum, it is the effect of temperature on shortening velocity that is the dominant factor determining the temperature-dependence of work output. Raising the temperature in this region increases shortening velocity and the net work done per cycle. At temperatures above the optimum, however, the effect of temperature on the time course of stretch activation and shortening deactivation becomes the major determinant of temperature-dependence. In this region, increasing temperature results in a reduction in the duration of both stretch activation and shortening deactivation. With increasing temperature, the periods of activation and deactivation become increasingly shorter than the shortening and lengthening portions of the strain cycle, more and more of the shortening and lengthening during a cycle occur outside the periods of most pronounced activation and deactivation, shortening work declines, lengthening work increases, and net work becomes smaller. The effect of increasing temperature on the time course of activation and deactivation is expected to become dominant sooner when the frequency of the strain cycle is low and the cycle duration long than when the frequency is high and the cycle duration short; hence, the shift in the optimum temperature to higher values as the strain frequency is increased (Fig. 17B,C).

Why was a temperature optimum not seen when the effects of changing temperature on work output were assayed at a single, fixed strain (Figs 15, 16)? In these experiments, the strain used was the optimal value at a muscle temperature of 30 °C. The optimal strain for work output increases with muscle temperature (Fig. 17A), and the strain that was optimal at 30 °C was presumably increasingly suboptimal as temperature was increased above 30 °C. Apparently, the negative effects of temperature increase on work output are reduced at suboptimal strain, but why this might be so remains to be worked out.

We thank R. D. Stevenson for the loan of an optical tachometer. This work was supported by NSF grant IBN9603187.

References

Abbott, R. H. and Steiger, G. J. (1977). Temperature and amplitude dependence of tension transients in glycerinated skeletal and insect fibrillar muscle. *J. Physiol., Lond.* **266**, 13–42.

Askew, G. N. and Marsh, R. L. (1997). The effect of length trajectory on the mechanical power output of mouse skeletal muscles. *J. Exp. Biol.* **200**, 3119–3131.

Bastian, J. and Esch, H. (1970). The nervous control of the indirect flight muscles of the honey bee. *Z. Vergl. Physiol.* **67**, 307–324.

Bauer, C. K. and Gewecke, M. (1985). Flight behaviour of the water beetle *Dysticus marginalis* L. (Coleoptera, Dytiscidae). In *Insect Locomotion* (ed. M. Gewecke and G. Wendler), pp. 205–214. Berlin: Verlag Paul Parey.

Bennett, A. F. (1984). Thermal dependence of muscle function. *Am. J. Physiol.* **247**, R217–R229.

Boettiger, E. G. (1957). Triggering of the contractile process in insect fibrillar muscle. In *Physiological Triggers* (ed. T. H. Bullock), pp. 103–116. Washington: American Physiological Society.

Boettiger, E. G. (1960). Insect flight muscles and their basic physiology. *Annu. Rev. Ent.* **5**, 1–16.

Buchthal, F., Kaiser, E. and Rosenfalck, P. (1951). The rheology of the cross striated muscle fibre. *Dan. Biol. Medd.* **21**, no. 7, 318pp.

Cullen, M. J. (1974). The distribution of asynchronous muscle in insects with particular reference to the Hemiptera: an electron microscope study. *J. Ent.* A **49**, 17–41.

Darwin, F. W. and Pringle, J. W. S. (1959). The physiology of insect fibrillar muscle. I. Anatomy and innervation of the basalar muscle of lamellicorn beetles. *Proc. R. Soc. Lond. B* **151**, 194–203.

Dudley, R. (1991). Comparative biomechanics and the evolutionary diversification of flying insect morphology. In *The Unity of Evolutionary Biology* (ed. E. C. Dudley), pp. 503–514. Portland: Dioscorides Press.

Dudley, R. (2000). *The Biomechanics of Insect Flight: Form, Function, Evolution*. Princeton: Princeton University Press.

Eisenberg, B. R. and Kuda, A. M. (1975). Stereological analysis of mammalian skeletal muscle. II. White vastus muscle of the adult guinea pig. *J. Ultrastruct. Res.* **51**, 176–187.

Ellington, C. P. (1991). Limitations on animal flight performance. *J. Exp. Biol.* **160**, 71–91.

Fawcett, D. W. and Revel, J. P. (1961). The sarcoplasmic reticulum of a fast-acting fish muscle. *J. Biophys. Biochem. Cytol.* **10**, 89–109.

Gewecke, M. (1975). The influence of the air-current sense organs on the flight behaviour of *Locusta migratoria*. *J. Comp. Physiol.* **103**, 79–95.

Gilmour, K. M. and Ellington, C. P. (1993a). Power output of glycerinated bumblebee flight muscle. *J. Exp. Biol.* **183**, 77–100.

Gilmour, K. M. and Ellington, C. P. (1993b). *In vivo* muscle length changes in bumblebees and the *in vitro* effects on work and power. *J. Exp. Biol*. **183**, 101–113.

Girgenrath, M. and Marsh, R. L. (1999). Power output of sound-producing muscles in the tree frogs *Hyla versicolor* and *Hyla chrysoscelis*. *J. Exp. Biol*. **202**, 3225–3237.

Granzier, H. L. and Irving, T. C. (1995). Passive tension in cardiac muscle: contribution of collagen, titin, microtubules and intermediate filaments. *Biophys. J.* **68**, 1027–1044.

Granzier, H. L. M. and Wang, K. (1993a). Interplay between passive tension and strong and weak binding cross-bridges in indirect flight muscle. *J. Gen. Physiol*. **101**, 235–270.

Granzier, H. L. M. and Wang, K. (1993b). Passive tension and stiffness of vertebrate skeletal and insect flight muscles: the contribution of weak cross-bridges and elastic filaments. *Biophys. J*. **65**, 2141–2159.

Helmes, M., Trombitás, K., Centner, T., Kellermayer, M., Labeit, S., Linke, W. A. and Granzier, H. (1999). Mechanically driven contour-length adjustment in rat cardiac titin's unique N2B sequence. *Circ. Res.* **84**, 1339–1352.

Ikeda, K. and Boettiger, E. G. (1965a). Studies on the flight mechanism of insects. II. The innervation and electrical activity of the fibrillar muscles of the bumblebee, *Bombus*. *J. Insect Physiol*. **11**, 779–789.

Ikeda, K. and Boettiger, E. G. (1965b). Studies on the flight mechanism of insects. III. The innervation and electrical activity of the basalar fibrillar muscle of the beetle, *Oryctes rhinoceros*. *J. Insect Physiol*. **11**, 791–802.

Josephson, R. K. (1973). Contraction kinetics of the fast muscles used in singing by a katydid. *J. Exp. Biol.* **59**, 781–801.

Josephson, R. K. (1985). Mechanical power output from striated muscle during cyclic contraction. *J. Exp. Biol*. **114**, 493–512.

Josephson, R. K. (1989). Power output from skeletal muscle during linear and sinusoidal shortening. *J. Exp. Biol*. **147**, 533–537.

Josephson, R. K. (1997a). Power output from a flight muscle of the bumblebee *Bombus terrestris*. II. Characterization of the parameters affecting power output. *J. Exp. Biol.* **200**, 1227–1239.

Josephson, R. K. (1997b). Power output from a flight muscle of the bumblebee *Bombus terrestris*. III. Power output during simulated flight. Characterization of the parameters affecting power output. *J. Exp. Biol.* **200**, 1227–1239.

Josephson, R. K. and Ellington, C. P. (1997). Power output from a flight muscle of the bumblebee *Bombus terrestris*. I. Some features of the dorso-ventral flight muscle. *J. Exp. Biol*. **200**, 1215–1226.

Josephson, R. K., Malamud, J. G. and Stokes, D. R. (2000). Asynchronous muscle: a primer. *J. Exp. Biol.* **203** (in press).

Josephson, R. K. and Stokes, D. R. (1999). The force–velocity properties of a crustacean muscle during lengthening. *J. Exp. Biol.* **202**, 593–607.

Josephson, R. K. and Young, D. (1981). Synchronous and asynchronous muscles in cicadas. *J. Exp. Biol*. **91**, 219–237.

Josephson, R. K. and Young, D. (1987). Fiber ultrastructure and contraction kinetics in insect fast muscles. *Am. Zool*. **27**, 991–1000.

Korschelt, E. (1923). *Bearbeitung einheimischer Tiere. Der Gelbrand* Dytiscus marginalis L. Leipzig: Verlag von Wilhelm Engelmann.

Linstedt, S. L., McGlothlin, T., Percy, E. and Pifer, J. (1998). Task-specific design of skeletal muscle: balancing muscle structural composition. *Comp. Biochem. Physiol*. **120**B, 35–40.

Machin, K. E. and Pringle, J. W. S. (1959). The physiology of insect fibrillar muscle. II. Mechanical properties of a beetle flight muscle. *Proc. R. Soc. Lond. B* **151**, 204–225.

Malamud, J. G. (1989). The tension in a locust muscle at varied muscle lengths. *J. Exp. Biol.* **144**, 479–494.

Malamud, J. G., Mizisin, A. P. and Josephson, R. K. (1988). The effects of octopamine on contraction kinetics and power output of a locust flight muscle. *J. Comp. Physiol.* A **162**, 827–835.

Marden, J. H. (1987). Maximum lift production during takeoff in flying animals. *J. Exp. Biol*. **130**, 235–258.

Mizisin, A. P. and Josephson, R. K. (1987). Mechanical power output of locust flight muscle. *J. Comp. Physiol.* A **160**, 413–419.

Mobley, B. A. and Eisenberg, B. R. (1975). Sizes of components in frog skeletal muscle measured by methods of stereology. *J. Gen. Physiol.* **66**, 31–45.

Molloy, J. E., Kyrtatas, V., Sparrow, J. C. and White, D. C. S. (1987). Kinetics of flight muscles from insects with different wingbeat frequencies. *Nature* **328**, 449–451.

Nachtigall, W. and Wilson, D. M. (1967). Neuro-muscular control of dipteran flight. *J. Exp. Biol.* **47**, 77–97.

Pringle, J. W. S. (1978). Stretch activation of muscle: function and mechanism. *Proc. R. Soc. Lond. B* **201**, 107–130.

Pringle, J. W. S. (1981). The evolution of fibrillar muscle in insects. *J. Exp. Biol*. **94**, 1–14.

Rome, L. C., Cook, C., Syme, D. A., Connaughton, M. A., Ashley-Ross, M., Klimov, A., Tikunov, B. and Goldman, Y. E. (1999). Trading force for speed: Why superfast crossbridge kinetics leads to superlow forces. *Proc. Natl. Acad. Sci. USA* **96**, 5826–5831.

Rome, L. C., Syme, D. A., Hollingworth, S., Lindstedt, S. L. and Baylor, S. M. (1996). The whistle and the rattle: The design of sound producing muscles. *Proc. Natl. Acad. Sci. USA* **93**, 8095–8100.

Schaeffer, P. J., Conley, K. E. and Lindstedt, S. L. (1996). Structural correlates of speed and endurance in skeletal muscle: the rattlesnake tail shaker muscle. *J. Exp. Biol.* **199**, 351–358.

Stellwaag, F. (1914). Der Flugapparat der Lamellicornier. *Z. Wiss. Zool.* **108**, 359–429.

Stevenson, R. D. and Josephson, R. K. (1990). Effects of operating frequency and temperature on mechanical power output from moth flight muscle. *J. Exp. Biol.* **149**, 61–78.

Swoap, S. J., Johnson, T. P., Josephson, R. K. and Bennett, A. F. (1993). Temperature, muscle power output and limitations on burst locomotor performance of the lizard *Dipsosaurus dorsalis*. *J. Exp. Biol.* **174**, 185–197.

Tregear, R. T. (1975). The biophysics of fibrillar flight muscle. In *Insect Muscle* (ed. P. N. R. Usherwood), pp. 357–403. London: Academic Press.

Unwin, D. M. and Ellington, C. P. (1979). An optical tachometer for measurement of the wing-beat frequency of free-flying insects. *J. Exp. Biol.* **82**, 377–378.

Usherwood, P. N. R. (1968). A critical study of the evidence for peripheral inhibitory axons in insects. *J. Exp. Biol.* **49**, 201–222.

White, D. C. S. (1983). The elasticity of relaxed insect fibrillar flight muscle. *J. Physiol., Lond.* **343**, 31–57.